Received: 10 March 2023 | Accepted: 17 August 2023

DOI: 10.1111/1365-2745.14201

Journal of Ecology | BRITISH ECOLOGICAL SOCIETY

RESEARCH ARTICLE

Fire-regime variability and ecosystem resilience over four millennia in a Rocky Mountain subalpine watershed

Kyra D. Clark-Wolf[1] | Philip E. Higuera[1] | Kendra K. McLauchlan[2] | Bryan N. Shuman[3] | Meredith C. Parish[4]

[1]Department of Ecosystem and Conservation Sciences, College of Forestry and Conservation, University of Montana, Missoula, Montana, USA

[2]Division of Environmental Biology, National Science Foundation, Alexandria, Virginia, USA

[3]Department of Geology and Geophysics, University of Wyoming, Laramie, Wyoming, USA

[4]Earth, Environmental, and Planetary Sciences, Brown University, Providence, Rhode Island, USA

Correspondence
Kyra D. Clark-Wolf
Email: kyra.clark-wolf@colorado.edu

Present address
Kyra D. Clark-Wolf, North-Central Climate Adaptation Science Center, Cooperative Institute for Research in Environmental Sciences, University of Colorado Boulder, Boulder, Colorado, USA

Funding information
National Science Foundation, Grant/Award Number: DEB-1655121, DEB-1655179 and DEB-1655189

Handling Editor: Guillaume de Lafontaine

Abstract

1. Wildfires strongly influence forest ecosystem processes, including carbon and nutrient cycling, and vegetation dynamics. As fire activity increases under changing climate conditions, the ecological and biogeochemical resilience of many forest ecosystems remains unknown.
2. To investigate the resilience of forest ecosystems to changing climate and wildfire activity over decades to millennia, we developed a 4800-year high-resolution lake-sediment record from Silver Lake, Montana, USA (47.360° N, 115.566° W). Charcoal particles, pollen grains, element concentrations and stable isotopes of C and N serve as proxies of past changes in fire, vegetation and ecosystem processes such as nitrogen cycling and soil erosion, within a small subalpine forest watershed. A published lake-level history from Silver Lake provides a local record of palaeohydrology.
3. A trend towards increased effective moisture over the late Holocene coincided with a distinct shift in the pollen assemblage c. 1900 yr BP, resulting from increased subalpine conifer abundance. Fire activity, inferred from peaks in macroscopic charcoal, decreased significantly after 1900 yr BP, from one fire event every 126 yr (83–184 yr, 95% CI) from 4800 to 1900 yr BP, to one event every 223 yr (175–280 yr) from 1900 yr BP to present.
4. Across the record, individual fire events were followed by two distinct decadal-scale biogeochemical responses, reflecting differences in ecosystem impacts of fires on watershed processes. These distinct biogeochemical responses were interpreted as reflecting fire severity, highlighting (i) erosion, likely from large or high-severity fires, and (ii) nutrient transfers and enhanced within-lake productivity, likely from lower severity or patchier fires. Biogeochemical and vegetation proxies returned to pre-fire values within decades regardless of the nature of fire effects.
5. *Synthesis*. Palaeorecords of fire and ecosystem responses provide a novel view revealing past variability in fire effects, analogous to spatial variability in fire severity observed within contemporary wildfires. Overall, the palaeorecord highlights ecosystem resilience to fire across long-term variability in climate and fire

activity. Higher fire frequencies in past millennia relative to the 20th and 21st century suggest that northern Rocky Mountain subalpine ecosystems could remain resilient to future increases in fire activity, provided continued ecosystem recovery within decades.

KEYWORDS
climate change, ecological resilience, fire regime, fire severity, lake-sediment record, palaeoecology, stable isotopes, subalpine forest

1 | INTRODUCTION

Wildfire activity is increasing across western North America, enabled in part by anthropogenic climate change (Abatzoglou & Williams, 2016; Kirchmeier-Young et al., 2017; Zhuang et al., 2021). In forests of the western United States, abundant fuels are expected to support continued climate-enabled increases in area burned through mid-century (Abatzoglou et al., 2021). Although fire is a long-standing process in these systems, altered fire regimes in concert with changing climate conditions can initiate vegetation transformations (Coop et al., 2020) and shifts in carbon (C) and nitrogen (N) cycling (Chen et al., 2017; Kelly et al., 2015; Walker et al., 2019), representing a loss of ecosystem resilience to fire (Seidl & Turner, 2022).

Resilience is a key organizing concept for understanding ecological change, defined as the capacity of an ecosystem to recover following a disturbance and retain fundamental processes, structures and species composition (Gunderson, 2000). While much of the literature on resilience has focussed on vegetation responses to disturbance (e.g. Blarquez & Carcaillet, 2010; Falk et al., 2022), system resilience emerges from both ecological and biogeochemical dynamics, encompassing processes operating on multiple timescales (Smithwick, 2011). Under historical conditions, many forest ecosystems exhibit resilience to fires (e.g. Carcaillet et al., 2010), with soil C and N typically recovering to pre-fire levels within years to decades alongside microbial and vegetation communities (Dunnette et al., 2014; Li et al., 2021). However, severe fires can create legacies in forest soils that persist for decades (e.g. Bowd et al., 2018), and shifts in fire regimes can alter slowly varying soil organic matter and nutrient pools (DeLuca & Sala, 2006; Pellegrini et al., 2020; Tierney et al., 2019). In turn, ecosystem modelling suggests that fire-induced N losses could constrain terrestrial productivity in global savanna biomes (Pellegrini et al., 2018); similar effects are also possible in forests (Toberman et al., 2014). Key uncertainties remain about the degree of coupling between vegetation and nutrient cycling in post-fire successional change (Dove et al., 2020; Hart et al., 2005), making it challenging to anticipate forest responses to changing fire activity in the context of ongoing climate change.

Fire frequency, behaviour and severity are key determinants of the magnitude and duration of fire effects on biogeochemical processes (Smithwick et al., 2005). Much of our understanding of the biogeochemical implications of fire-regime change comes from long-term experiments or spatial comparisons in ecosystems that have historically experienced frequent, low-severity fires (i.e. fires that do not kill the majority of trees, once every few years to decades on average). In contrast, in ecosystems historically characterized by infrequent, high-severity fires (i.e. fires that kill the majority of trees, once every century or more on average), the implications of fire-regime changes are less well-constrained due to a lack of long-term empirical datasets. High-resolution palaeoecological records help fill this knowledge gap by resolving the effects of individual disturbances (e.g. Blarquez & Carcaillet, 2010), which ultimately scale up to shape ecosystem changes over millennia, highlighting the potential for both long-term variation and stability in ecosystem dynamics (Carcaillet et al., 2020; Hudiburg et al., 2017). Such retrospective information provides context for anticipating the effects of anthropogenic climate change and shifting fire regimes on element cycling in ecosystems characterized by infrequent, high-severity fire regimes.

Existing palaeoecological records reveal diverse impacts of wildfires on terrestrial and aquatic ecosystems, leaving signals integrated through proxies measured in lake sediments. For example, high-severity fires in a subalpine forest in Colorado resulted in losses of N, S and base cations (Ca, K and Mg) from the terrestrial environment through volatilization and enhanced postfire erosion, followed by re-accumulation over several decades during forest aggradation (Dunnette et al., 2014; Leys et al., 2016). However, records from other subalpine forests and boreal regions reveal a variety of post-fire changes in lake-sediment geochemistry (Chipman & Hu, 2019; Pompeani et al., 2020), arising in part from differences in topography, organic matter sources and sample resolution (Morris et al., 2015). Varying ecosystem responses to fire have not been observed within a single multi-millennial record, making it challenging to separate the relative influences of site characteristics, fire severity and longer-term climatic- or fire-regime change on ecosystem processes.

In the present study, we evaluate decadal-scale biogeochemical and vegetation responses to fire (i.e. 'fire–ecosystem dynamics'), within the context of long-term climatic change over recent millennia. We use a lake-sediment record from the U.S. northern Rocky Mountains to investigate two questions: (1) how do vegetation and biogeochemical processes respond to wildfires over successional timescales; and (2) how do these ecosystem responses to fire vary over periods of directional climate change in past millennia? Here, we summarize biogeochemical and vegetation responses to wildfires

using a simple definition of resilience: recovery of a response variable to pre-fire levels, within a time period shorter than the average fire return interval (FRI; McLauchlan et al., 2014; Napier & Chipman, 2022). We hypothesize that recovery of biogeochemical processes consistently occurs within decades after fire due to close coupling with forest succession, supporting ecosystem resilience to individual fires. We further hypothesize that fire–ecosystem dynamics are sensitive to climate, directly or indirectly, such that long-term changes in climate and vegetation communities over millennia would alter decadal-scale ecosystem responses through shifts in fire frequency, fire effects (i.e. fire severity) and/or postfire recovery times (e.g. fig. 5a, McLauchlan et al., 2014). Alternatively, a lack of variation in ecosystem responses to individual fires would indicate low sensitivity of fire–ecosystem dynamics to climatic changes experienced in recent millennia. The result of a directional trend in climate thus may be long-term stability, or a 'stair step' biogeochemical trend due to changes in fire–ecosystem dynamics (fig. 5b, McLauchlan et al., 2014).

To investigate these hypotheses, we developed a 4800-year multiproxy biogeochemical, vegetation and fire-history record from Silver Lake, Montana, USA. Silver Lake is situated in a subalpine forest watershed in the northern Rocky Mountains, and a published lake-level reconstruction from this site provides a local palaeohydrology record (Parish et al., 2022). This represents a rare pairing of co-located palaeoecological and palaeoclimate reconstructions, which allows us to build on and extend prior work by testing the effects of long-term climatic change on decadal-scale ecosystem impacts of past fires. A suite of biogeochemical proxies with decadal resolution integrates both direct (e.g. combustion and volatilization) and indirect (e.g. postfire erosion and revegetation) effects of fire on C and nutrient pools. We draw comparisons between the late Holocene record described here and changes expected over the 21st century to help anticipate the potential resilience of subalpine forest ecosystems to shifting climate and wildfire activity.

1.1 | Study area and site description

Silver Lake is located in the northern Bitterroot Mountains in the Lolo National Forest, Montana, USA (Figure 1). The lake has a surface area of 5.26 ha and a maximum water depth of 18.8 m. Silver Lake lies at 1623 m elevation in a c. 100-ha cirque basin dammed by a glacial moraine, with no significant inlet streams and a seasonal outlet. The lake basin lies on the Proterozoic Wallace Formation, composed of dolomitic quartzite and siltite capped by black argillite, and is locally intersected by diorite (Vuke et al., 2007). Soils in the watershed are deep, well-drained andisols and inceptisols derived from glacial till overlain by volcanic ash, both of which were deposited since the Last Glacial Maximum ~18,000 years ago (USDA-NRCS, 2019).

Subalpine forests in the Silver Lake watershed are dominated by *Abies lasiocarpa* (Hook.) Nutt. (subalpine fir) and *Picea engelmannii* Parry ex Engelm. (Engelmann spruce), with smaller components of

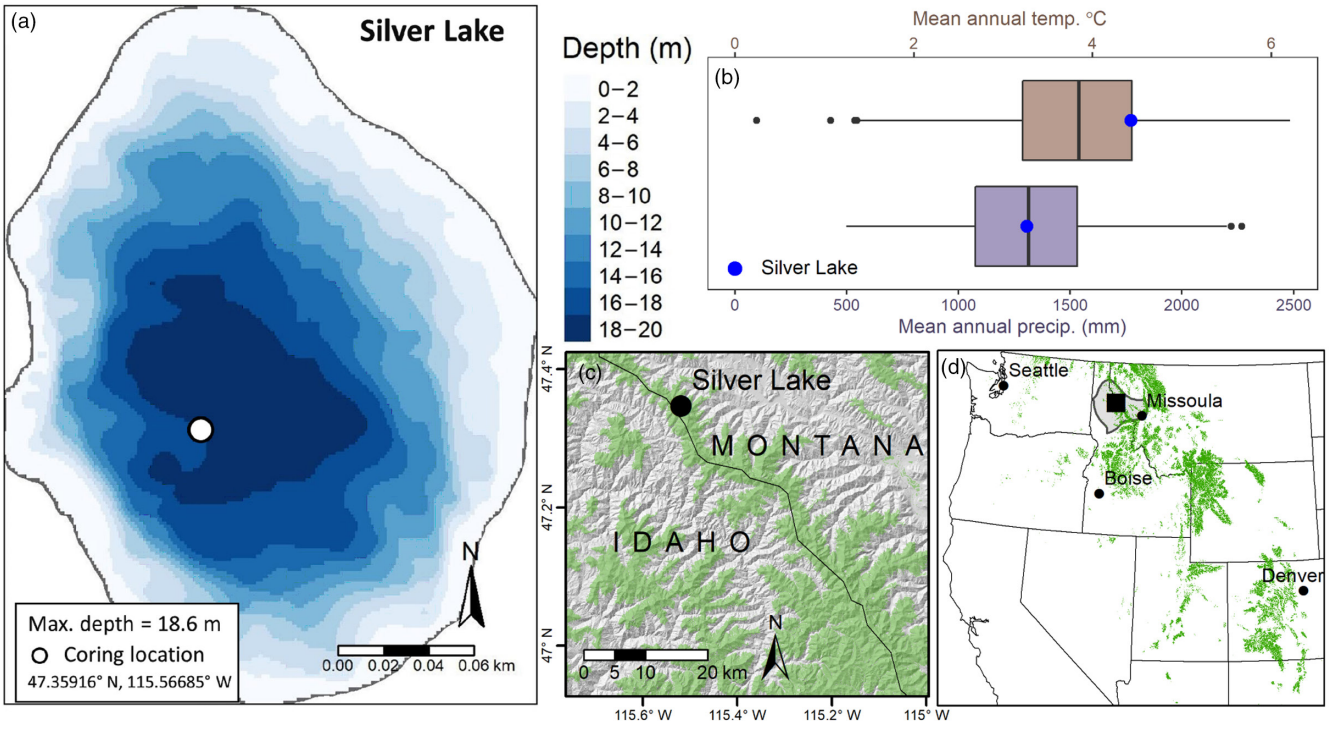

FIGURE 1 Location, climate and bathymetry of Silver Lake. (a) Bathymetry of Silver Lake, with coring location. (b) Regional climate (30-year normal of mean annual temperature and total precipitation) for subalpine forests within the Bitterroot Mountains ecoregion (grey outline in (d); Bailey, 1995), compared with the climate of Silver Lake (blue dot). (c, d) Location of Silver Lake near the Idaho-Montana state line. The green area delineates the potential extent of Rocky Mountain subalpine forest based on LandFire Environmental Site Potential (landfire.gov). The location of the study area is represented by a square in (d), with the Bitterroot Mountains ecoregion shown in grey.

Tsuga mertensiana (Bong.) Carriere (mountain hemlock), *Pinus contorta* Dougl. var. *latifolia* Engelm. (lodgepole pine) and *Larix occidentalis* (western larch). Broadleaf taxa are not a significant component of subalpine forests in the region. Alder trees (*Alnus rubra* Bong.) and shrubs (*Alnus viridis* ssp. *sinuata* (Regel) Love & Love) are common within the region in riparian and disturbed areas, respectively. The site burned most recently in 1918 CE, but not in the regionally extensive fire year of 1910 (Gibson et al., 2014). Total annual precipitation averaged 1307 mm ± 197 (SD), and mean annual temperature averaged 4.4°C ± 0.7 from 1981 to 2010 (PRISM Climate Group, 2021). Precipitation is snow-dominated, with melt-off typically occurring in June in high-elevation areas. The fire season is most active during the driest months of July and August, during which an average of less than 50 mm of rain falls.

Palaeohydrology in the study region is well-resolved by a lake-level reconstruction from Silver Lake itself (Parish et al., 2022). The record provides evidence of increasing effective moisture c. 2800 calendar years before present (hereafter yr BP, with present defined as 1950 CE), with modern lake levels reached c. 1800 yr BP. Coincident shifts in vegetation at regional sites corroborate the timing of hydroclimate changes at Silver Lake (Figure S2).

2 | MATERIALS AND METHODS

2.1 | Lake-sediment sampling

Permission to collect sediment cores was given by the Lolo National Forest and did not require a formal permit. Two overlapping sediment cores were collected from the deepest part of the lake in September 2017 using a 7.62-cm diameter, modified Livingstone piston corer (Wright et al., 1984). A total of c. 8 m of sediment were recovered, terminating in a thick tephra layer inferred to be the Mount Mazama tephra (c. 7631 cal yr BP; Egan et al., 2015). A short core was collected in June 2018 using a polycarbonate tube piston corer, and the upper c. 30 cm of sediment was extruded vertically in the field at 0.5-cm intervals. Deeper cores were extruded horizontally in the laboratory, split lengthwise and photographed.

The record was characterized by uniform dark brown gyttja with fine laminations in the uppermost c. 21 cm and intermittent laminations throughout the deeper sediments. Cores were correlated based on visual stratigraphy and combined with overlapping sections to produce a continuous record. Cores were sliced at 0.5-cm intervals for subsequent proxy development.

2.2 | Chronology

Sediment ages were inferred based on measurements of ^{210}Pb activity in 15 samples spanning the upper 40 cm of sediments, AMS ^{14}C from terrestrial macrofossils or charcoal in 14 samples from deeper sediments and three estimated ages of tephra layers (Table S1). Measurements of ^{210}Pb activity were obtained from Flett Research Ltd. (Manitoba, Canada), and two measurements of ^{226}Ra activity were used to confirm supported ^{210}Pb activity. Ages were estimated using the constant rate of supply model (Binford, 1990). Tephra layers were identified visually, and ages were inferred based on known tephra deposits at Silver Lake (Parish et al., 2022). Radiocarbon dating was conducted at the Lawrence Livermore National Laboratory's Center for Accelerator Mass Spectrometry, and ^{14}C ages were calibrated using IntCal20 (Reimer et al., 2020). An age–depth relationship was built using the package *rbacon* in R (v. 4.1.1, R Core Team, 2021), with flexible priors to allow a range of sediment accumulation rates (Figure S1; Blaauw & Christen, 2011).

2.3 | Vegetation history

Local vegetation change at Silver Lake was inferred from pollen analyses from 54 sediment samples within the past 5000 years, corresponding to one sample every 96 years on average (SD = 36). Subsamples were processed using standard methods (Fægri et al., 1989), and pollen was counted at 400x magnification (EMH Consulting, LLC). Pollen was identified to the lowest taxonomic level possible using keys (Fægri et al., 1989; Kapp et al., 2000) and the modern reference collection at the University of Oregon. A minimum of 300 terrestrial pollen grains were identified in each sample, averaging 366 grains (SD = 16). Although *A. lasiocarpa* and *A. grandis* are both present in our study area, they are not distinguished based on pollen. *Cyperaceae* was excluded from pollen sums due to its high abundance in some samples (up to 90%), likely originating from wetland taxa along the lake margin. Pollen concentration was determined by adding a known concentration of an exotic tracer (*Lycopodium*) and used to calculate pollen accumulation rate (PAR).

Pollen abundances were summarized as percentages of the terrestrial sum. Pollen types present in at least 50% of samples and with a maximum abundance of at least 1% were considered major taxa (Chileen et al., 2020); these taxa were further grouped into three categories: conifer (trees), broadleaf (trees and shrubs) and herbaceous (understory grasses and forbs). Pollen percentages were used to calculate squared-chord distances, and a stratigraphically constrained clustering analysis using the CONISS method was applied to identify distinct pollen zones (*rioja* package in R). The relative proportion of overstory-to-understory taxa (AP:NAP) was calculated using the equation $[a-b]/[a+b]$, where a is the sum of arboreal pollen counts (conifer and deciduous) and b is the sum of nonarboreal pollen counts (shrubs and herbaceous plants), to yield an index that is symmetric and bounded between −1 and 1 (e.g. Chileen et al., 2020; Jiménez-Moreno et al., 2011). We calculated a conifer-to-broadleaf pollen ratio (conifer: broadleaf) using the same equation.

To assess decadal-scale vegetation responses to fire, each pollen sample was classified based on time-since-fire. Pollen percentages of each sample reflect the average plant assemblage over the period recorded by the 0.5-cm sediment slice (c. 5 years, the median sample resolution). Time-since-fire values were determined as the age difference between the sediment sample from which pollen was

extracted and the closest prior sediment sample with an identified charcoal peak (Chileen et al., 2020); see below for charcoal peak detection methods. Pollen samples that were within 10 years before a charcoal peak or up to 40 years after were considered fire-coincident ('fire', $n = 15$), to account for potential imprecision in identifying the exact timing of charcoal peaks (which can span multiple samples). We interpret these samples as generally reflecting the short-term (first- and second-order) fire effect on the plant assemblages. These fire-coincident samples were compared with 'nonfire' samples, from 41 to 80 years ($n = 7$), 81 to 120 years ($n = 11$) and >120 years ($n = 20$) after charcoal peaks. We interpret these samples as reflecting postfire successional changes in vegetation assemblages. Pollen percentages and ratios from among these four sets of samples were compared using nonparametric Wilcoxon rank-sum and Kruskal–Wallis tests to evaluate differences in the median abundances of major pollen taxa following fires.

2.4 | Fire history

For charcoal analysis, sediment subsamples of 3 cm^3 were taken from continuous 0.5-cm slices and soaked in a 5% sodium metaphosphate solution for 72 h before gently wet sieving through a 125-μm wire mesh sieve. Samples were soaked in a 2% sodium hypochlorite solution for an additional 24 h and sieved again, and charcoal particles were identified visually under a stereomicroscope and counted at 10–40× magnification.

The time series of charcoal accumulation rates was analysed using *CharAnalysis* (Higuera, 2009) in MATLAB (MathWorks, 2021) to identify distinct peaks that were inferred as local fire events (i.e. one or more fires within c. 500–1000 m of the lake during the 10-year sampling interval) (Whitlock & Larsen, 2001). Prior to peak detection, charcoal concentrations (pieces cm^{-3}) were interpolated to a constant timestep of 10 years and multiplied by sediment accumulation (cm $year^{-1}$) to calculate charcoal accumulation rate (CHAR, pieces cm^{-2} $year^{-1}$). Low-frequency trends in CHAR ('background') were estimated with a 500-year locally weighted regression robust to outliers (Cleveland, 1979), which was subtracted from the CHAR time series to produce a residual time series. Peaks in residual CHAR that exceeded the 99th percentile of a locally fit Gaussian mixture model were identified and screened using a minimum-count test; a charcoal peak was interpreted as a fire if it had less than a 5% probability of coming from the same Poisson distribution as the minimum charcoal count within the prior 75 years.

We used the identified charcoal peaks to characterize the frequency component of the fire regime within two time periods, defined based on pollen zones. The timing of fire events was used to calculate FRIs, and the mean fire return interval (mFRI) was summarized for each zone. We estimate 95% confidence intervals around the mFRI from 1000 bootstrapped samples of FRIs within each zone. To detect potential changes in fire regimes, a two-parameter Weibull model was fit to the FRIs from each zone using maximum likelihood techniques (*fitdistrplus* package in R). Weibull models are commonly used to describe fire-interval distributions, which are not expected to be normally distributed (Johnson & Gutsell, 1994). Goodness-of-fit between the Weibull model and empirical distribution was assessed using a one-sample K-S test. We tested the null hypotheses that the distribution of FRIs did not differ between zones using a likelihood ratio test following methods described by Higuera et al. (2009).

2.5 | Sediment biogeochemistry

We selected a suite of biogeochemical proxies to characterize the site context and investigate decadal-scale fire effects on watershed processes such as nutrient loss and retention. To infer terrestrial and aquatic ecosystem responses to fire, we used multiple proxies that reflect variations in whole-ecosystem N availability ($\delta^{15}N$), sediment organic matter composition and origin (C, N, C:N and $\delta^{13}C$), transfers of base cations and other lithogenic minerals from the terrestrial environment to the lake (Ti, K, Ca, Al, Si, Mg, P and S) and within-lake dynamics (Fe and Mn). Interpreted together, these variables integrate N-cycle dynamics, terrestrial and aquatic organic matter inputs and processing, and allochthonous clastic detritus from soil erosion, providing information about watershed processes difficult to distinguish from individual proxies alone (Boyle, 2001; Meyers, 1997; Talbot, 2001). Here, we briefly highlight links with primary biogeochemical signals that inform our selection and use of these proxies. Sedimentary $\delta^{15}N$ values integrate ecosystem N availability, with higher values resulting from a more 'open' N cycle with greater fractionating N losses, and low values representing greater N conservation, such as during forest aggradation (Robinson, 2001; Vitousek & Reiners, 1975). Sedimentary $\delta^{13}C$ often correlates with lake productivity (Brenner et al., 1999), while C:N provides a proxy for the relative contributions of algal (values c. 4–10) versus terrestrial organic matter (values >20; Meyers & Teranes, 2001). Ti is biologically inert, and it is used here as a proxy for clastic detritus from soil erosion (Davies et al., 2015); this interpretation of Ti is corroborated by variation in concentrations of other rock-derived elements. Redox-sensitive elements, such as Mn and Fe (or their ratio), provide an indication of redox conditions in the water column or upper sediments (Davies et al., 2015). Although interpretations of elements with multiple potential origins are more ambiguous (e.g. rock-derived vs. biogenic silica), we included these in our analysis to fully characterize the sediment composition.

Biogeochemical proxies were analysed from each 0.5-cm-interval sample spanning the past c. 4800 years, totalling 861 samples. Subsamples of 0.5–1 cm^{-3} were oven dried at 65°C for at least 48 h and homogenized. Dried samples were weighed prior to geochemical analyses to calculate bulk density (g dry mass cm^{-3}). The concentrations of 10 major elements (Al, Ca, Fe, K, Mg, Mn, P, S, Si and Ti) were measured using X-ray fluorescence (XRF) at the Paleoenvironmental Lab at Kansas State University. Samples were measured using a handheld Bruker Tracer 5i wavelength-dispersive XRF analyzer for 300 s, and the concentration of each element (% dry mass) was calculated using a soil

calibration. Analytical precision was estimated by conducting at least three repeat measurements on a set of 60 samples spanning the core, with an average coefficient of variation of approximately 3%–9%.

Sediment C, N and isotopic composition were measured on the same sediment samples using a Costech 4010 Elemental Analyzer and a Thermo Finnigan Delta V Plus XP mass spectrometer at the University of Wyoming Stable Isotope Facility. Sediment C and N are reported in % dry mass. Isotope ratios are reported relative to VPDB for carbon and atmospheric N_2 for nitrogen, using standard delta notation ($\delta^{13}C$, $\delta^{15}N$, ‰). Analytical precision was estimated via repeat measurements for 56 samples spanning the core. Precision was ±0.07‰ and ±0.04‰ for $\delta^{15}N$ and $\delta^{13}C$, and ±0.14% and ±0.01% for C and N, respectively. A correction was applied to $\delta^{13}C$ measurements younger than 1800 CE to account for the Suess effect (Dombrosky, 2020).

2.6 | Statistical analyses of biogeochemical proxies

Dominant modes of variation in elemental concentrations and isotopic composition of sediments (C, N, S, P, Ca, K, Al, Ti, Si, Mg, C:N, $\delta^{13}C$ and $\delta^{15}N$) were summarized via a principle component analysis (PCA) using the *ade4* package in R (Dray & Dufour, 2007). Biogeochemical data were log-transformed prior to PCA as needed to reduce skewness, based on a visual inspection of histograms. Row weights were used to ensure that the influence of each sample was equally distributed across sample ages.

To quantify the impacts of individual fire events on sediment geochemistry, we used a compositing technique derived from superposed epoch analysis (Dunnette et al., 2014; Genries et al., 2009). Biogeochemical proxies were interpolated to 10-year timesteps, detrended and averaged over a pre-fire baseline of 20–40 years before each charcoal peak and again over 0–20, 30–50 and 60–80 years after each charcoal peak. To produce a composite record summarizing changes in biogeochemical proxies before and after fire events, values in each time lag were averaged across all inferred fire events in the record. A Monte Carlo randomization method was used to generate confidence intervals for the mean response (Appendix S1), and significance is reported using a 'language of evidence' (Muff et al., 2021).

Upon initial inspection of the composite records, at least two distinct patterns emerged. To quantify and evaluate the robustness of these patterns, a posteriori, we used hierarchical cluster analysis to identify sets of fire events with similar postfire biogeochemical patterns. For each fire event, values of each element or isotope were extracted and averaged over 0–30 years and over 40–70 years following a fire; this differed from the compositing described above, to avoid excess complexity while capturing the initial magnitude and the duration of responses. Postfire averages for each variable were scaled (by *z*-scores) and used to calculate squared-chord distances among all fire events. A hierarchical cluster analysis using Ward's minimum variance method was performed, a commonly used agglomerative clustering method based on a sum-of-squares criterion (Murtagh & Legendre, 2014), identifying two distinct sets of postfire responses. We termed the two distinct patterns of postfire biogeochemical responses 'erosion-associated' (Type 1, $n = 10$) and 'nonerosional' (Type 2, $n = 10$) based on differences in postfire concentrations of lithogenic minerals such as Ti (Figure 6; cf. Leys et al., 2016). For consistency, we use these terms throughout; see Discussion for details on the interpretation of biogeochemical responses to fire events.

Finally, given the expectation that some charcoal peaks recorded in sediment records result from low-severity or extra-local fires, and thus would not influence catchment biogeochemistry (Dunnette et al., 2014), we conducted an additional step to identify fires with no detectable biogeochemical response (Appendix S1). Fire events that lacked a significant biogeochemical response were removed from each cluster and placed into an additional category, 'nonresponsive'. To characterize the average biogeochemical impacts of these different populations of fire events, we conducted separate composite analyses, as described above, using each of the three distinct sets of fire events.

3 | RESULTS

3.1 | Chronology

The Silver Lake record extends to c. 4800 yr BP. Each ½-cm sample represents a median of 5 years (range: 1–18), corresponding to a median sediment accumulation rate of 0.13 cm $year^{-1}$ (Figure 2). Although the core retrieved extends to deeper and older sediment, we restricted our analyses to sediments younger than 4800 yr BP, due to a distinct increase in sediment accumulation rate over approximately 500–600 cm depth, relative to the rest of the core (Figure S1).

3.2 | Vegetation history

Pollen assemblages were dominated by coniferous tree taxa (Figure 3), with a median abundance of major conifer taxa of 70% (interquartile range, IQR: 64%–77%) over the past 4800 years, with 35% (33%–40%) from *Pinus* pollen types (Figure 3). Diploxylon *Pinus* pollen types are interpreted as originating from *P. contorta* (or possibly long-distance transport of *P. ponderosa*), while haploxylon pollen types are interpreted as originating from *P. albicaulis* or *P. monticola*. *Abies* pollen types (interpreting as originating from *A. lasiocarpa* or *A. grandis*) and *Picea* pollen types (*P. engelmannii*) had median abundances of 11% (IQR: 10%–15%) and 12% (8%–16%), respectively. *Pseudotsuga-Larix*-type, *Tsuga*, and Cupressaceae pollen types each had median abundances of <5%. Among nonconifer taxa, *Alnus rubra* pollen types were the most abundant, with a median of 14% (9%–16%). Dominant pollen types from understory taxa included *Alnus viridis* ssp. *sinuata*, Poaceae and *Artemisia*, each averaging 3% abundance.

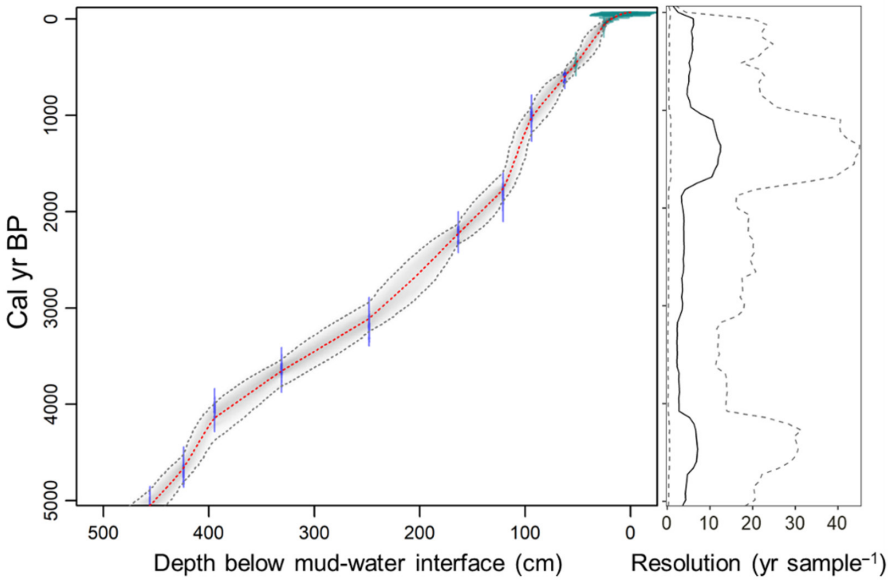

FIGURE 2 Age–depth relationship over the past 5000 years for the Silver Lake record, modelled using *rbacon*. Purple bars show the distribution of calibrated ages for radiocarbon dates, while green shows additional dates (tephra layers and Pb^{210}-inferred ages). The red curve is the median estimated age for each depth, and the shaded area shows the 95% confidence intervals. Average sample resolution with confidence intervals is shown on the right.

Millennial-scale changes in pollen abundance were summarized using cluster analysis, which revealed one significant shift in the pollen assemblage at c. 1900 yr BP (Figure 3). At Silver Lake, the AP:NAP index was relatively constant over millennial timescales, averaging 0.75 (IQR: 0.66–0.81), but the relative abundances of arboreal pollen taxa shifted (Figure 3). *Pinus* pollen types increased in abundance from a median of 34% between 4800 and 1900 yr BP to 41% after 1900 yr BP ($p < 0.001$), in part driven by an increase in haploxylon-type pollen from 1% to 4%. Concurrently, median abundance of *T. mertensiana* and *Abies* pollen types increased from 1% to 3% ($p < 0.001$) and from 11% to 14% ($p = 0.03$), respectively, while percentages of *Alnus rubra* and *Alnus viridis* ssp. *sinuata* pollen types decreased from 19% to 8% median abundance ($p < 0.001$) and from 5% to 2% ($p = 0.002$), respectively.

3.3 | Fire history

Charcoal particles were abundant throughout the 4800-year record, with a median concentration of 25 charcoal pieces cm^{-3} and median accumulation rate of 2.4 pieces $cm^{-2}year^{-1}$. The record-wide median signal-to-noise index was 4.3 (range: 3–10, Figure S3), indicating the suitability of the record for charcoal peak analysis (cf. Kelly et al., 2011). Charcoal peak analysis identified 31 peaks over the past 4800 years (Figure 3), interpreted as local fire events. Zone 2 included a period lacking charcoal peaks from c. 3000 to 2500 yr BP, which may represent a true fire-free interval, or may include undetected fires that were too small or low severity to register as charcoal peaks in the sediment record (Appendix S2). mFRIs for Zones 1 (1900 yr BP–present) and 2 (4760–1900 yr BP) were 223 years (95% CI: 175–280) and 126 years (83–184), respectively. A likelihood ratio test provided moderate evidence that the FRI distribution in Zone 1 differed from Zone 2 ($p = 0.02$, Table S2). This represents a significant decrease in fire frequency after 1900 yr BP, reflecting a 77% lengthening of the mFRI.

3.4 | Biogeochemical proxies and millennial-scale variation

Sediments were moderately organic, with median C and N concentrations of 16% (interquartile range, IQR: 13.6%–17.2%) and 1.1% (1.0%–1.2%), respectively (Figure 4). The median molar C:N ratio of 14.4 (IQR: 13.5–15.3) was lower than the C:N of terrestrial soil and foliar samples from the surrounding watershed (median 18.8 and 43.9, respectively; Figure S4). Stable isotope values of C and N and their concentrations varied independently. Sedimentary $\delta^{15}N$ values averaged 0.65‰ (IQR: 0.46–0.85‰), intermediate between the average $\delta^{15}N$ of mineral soil and foliage (Figure S4), and varied only slightly throughout the record. Sedimentary $\delta^{13}C$ values averaged −27.6‰ (IQR: −29.8 to −26.7‰) and varied as much as 3–5‰ over multidecadal timescales throughout the record (Figure 4).

Sedimentary element concentrations and isotopes exhibited notable low-frequency variability, summarized by PCA. Principal components 1 and 2 (PC1 and PC2) together explained 67.6% of the variability in biogeochemical proxies (Figure 5). Millennial-scale trends were characterized by applying a 1000-year loess smoother to PC1 and PC2 (Figure 5). PC1 accounted for 42.2% of the variability and was positively associated with $\delta^{13}C$, $\delta^{15}N$, C:N and concentrations of rock-derived elements and base cations (K, Si, Ti and Ca). PC1 was negatively associated with concentrations of redox-sensitive elements and those associated with organic matter, including C, N, P, S, Fe and Mn. PC1 reached a maximum at c. 2500 yr BP and generally declined towards present, broadly reflecting a long-term decline in $\delta^{13}C$ values and concentrations of several rock-derived elements (e.g. Ti and Ca) and a distinct increase in concentrations of P, S, Mn and Fe after c. 2500 yr BP. PC2 accounted for 25.4% of the variability and was positively correlated with Mg, reflecting an antiphase between Mg concentrations compared with Al and other elements. PC2 varied

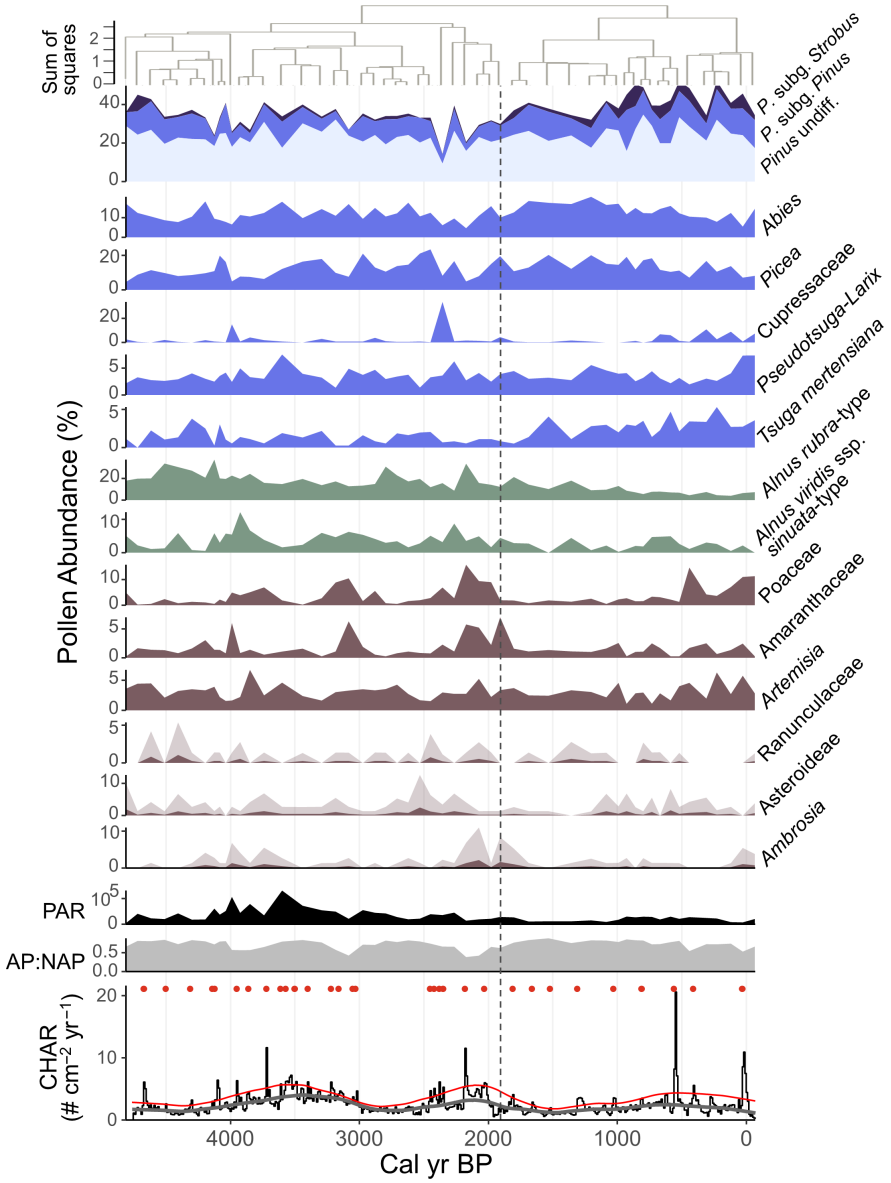

FIGURE 3 Pollen and charcoal records, showing per cent abundance of major pollen taxa, pollen accumulation rate (PAR, grains cm^{-2} year^{-1}), the ratio of arboreal to nonarboreal pollen (AP:NAP) and the charcoal accumulation rate (CHAR, pieces cm^{-2} year^{-1}). The results of hierarchical cluster analysis are displayed, with two significant pollen zones identified and delineated using a dashed line (break at 1909 yr BP). The shaded area on the bottommost three pollen panels shows a 5× magnification of pollen percentages, to highlight changes over time in taxa with low abundance. Colours denote major pollen types (blue = coniferous trees; green = broadleaf trees and shrubs; brown = herbaceous understory plants). The grey and red curves on the CHAR panel display 500-year smoothed estimates of background CHAR and the threshold used in peak analysis, respectively; red dots correspond to charcoal peaks exceeding the threshold. The transition between pollen zones also corresponded to a significant shift in charcoal peak frequency. Pollen types are as follows: *Pinus* (pine, separated into subgenus *Strobus*, subgenus *Pinus* and undifferentiated pollen types), *Abies* (fir), *Picea* (spruce), Cupressaceae (cypress family), *Pseudotsuga-Larix* (genera of larch and Douglas-fir), *Tsuga mertensiana* (mountain hemlock), *Alnus rubra*-type (red alder), *Alnus viridis* ssp. *sinuata*-type (green alder), Poaceae (grass family), Amaranthaceae (amaranth and goosefoot family), *Artemisia* (sagebrush), Ranunculaceae (buttercup family), Asteroideae (aster subfamily) and *Ambrosia* (ragweed).

throughout the record, increasing modestly between c. 4800 and 3600 yr BP and decreasing slightly between c. 2200 and 700 yr BP. Variation in biogeochemical proxies also manifested on centennial timescales, notably a distinct decline in C and N during a long fire-free interval from c. 3000 to 2400 yr BP.

3.5 | Decadal-scale ecosystem responses to fire

Ecosystem responses to individual fires did not differ before and after the fire-regime shift c. 1900 yr BP. Two categories of distinct post-fire biogeochemical responses were identified in the record, each

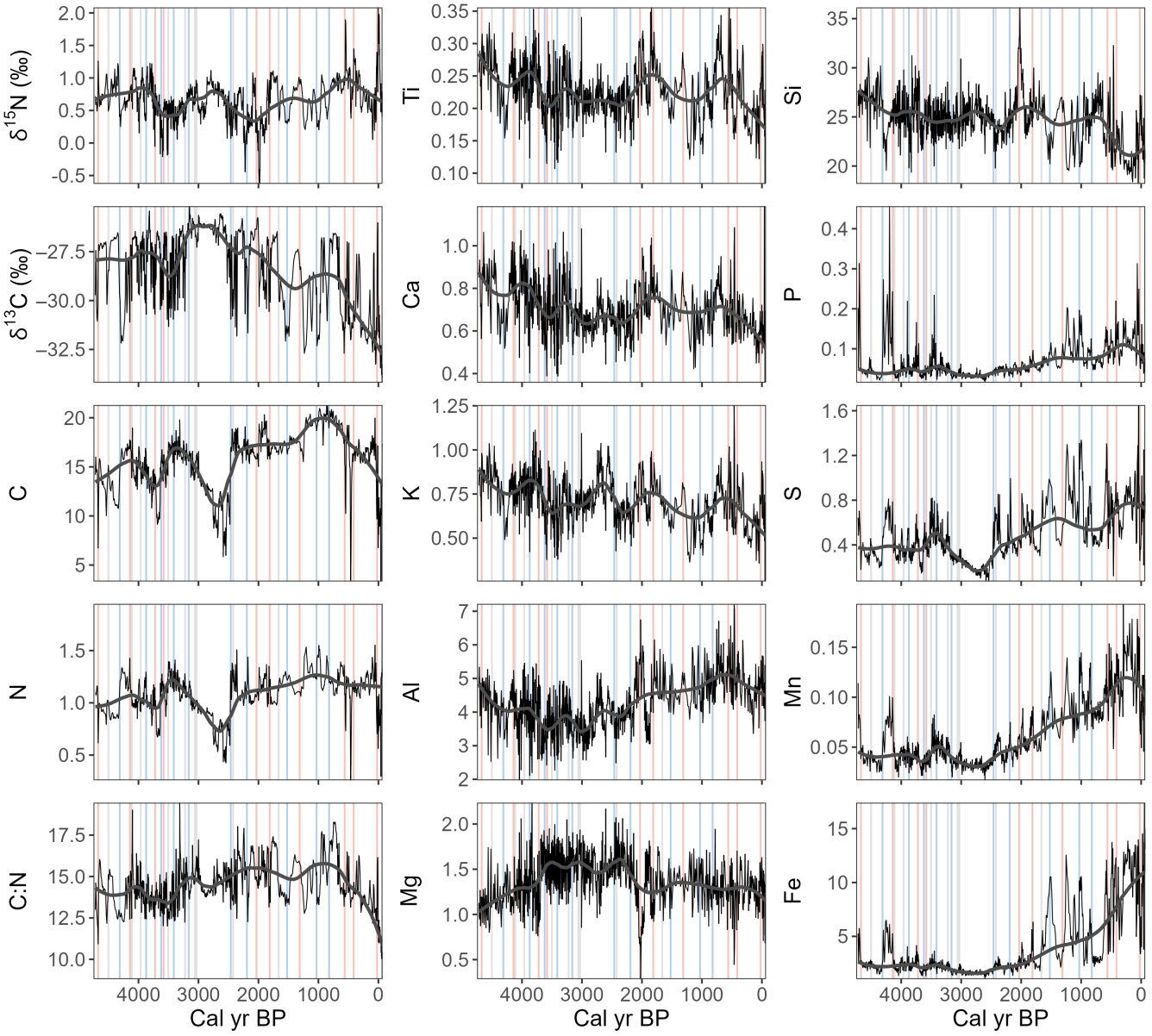

FIGURE 4 Time series of sedimentary isotope values ($\delta^{13}C$ and $\delta^{15}N$, ‰), C:N values and element concentrations (%), showing high-frequency variation and low-frequency (1000-year) trends using a loess smoother robust to outliers. Vertical lines denote the timing of inferred fire episodes, with red for Type 1 (erosion-associated) fires, blue for Type 2 (nonerosional) fires and grey for nonresponsive fires.

of which was composed of similar numbers of fire events: 'erosion-associated' (Type 1, $n = 10$), and 'nonerosional' (Type 2, $n = 10$), with a third category lacking detectable biogeochemical impacts, 'non-responsive' ($n = 9$). Each of these three postfire response types occurred consistently throughout the record (Figure S5).

The average response following erosion-associated (Type 1) fires was characterized by an initial increase in the concentrations of lithogenic elements (Figure 6). The composite analysis for erosion-associated fires showed strong evidence of an increase in mean values of Ti, $\delta^{15}N$, Al, K and Si and a decline in C relative to the long-term average over 0–20 years after fire ($p < 0.01$). These patterns are summarized by an increase in PC1 and a decrease in PC2 values relative to pre-fire samples, reflecting overall changes in sediment composition following fire. There was moderate evidence of initial increases in sediment bulk density, Ca, and $\delta^{13}C$, and a decline in N over 0–20 years following fire events ($p < 0.05$), although the responses in C, N, $\delta^{13}C$, Al, K, Si and Ca were not significant when medians were considered (Figure 6). Geochemical responses following these erosion-associated fire events persisted for 30–50 years for all proxies except $\delta^{15}N$ and C, which returned to pre-fire values on average within c. 20 years after fire. All geochemical responses were recovered to baseline or reversed in sign by 60–80 years after fire.

The average response following nonerosional (Type 2) fires was characterized by opposing responses in many proxies compared with erosion-associated (Type 1) fires (Figure 6). There was strong evidence of an initial increase in sediment N concentration and a decrease in Ti, $\delta^{13}C$, $\delta^{15}N$, C:N, sediment bulk density, Al, K and Ca 0–20 years after nonerosional fires ($p < 0.01$), summarized by an

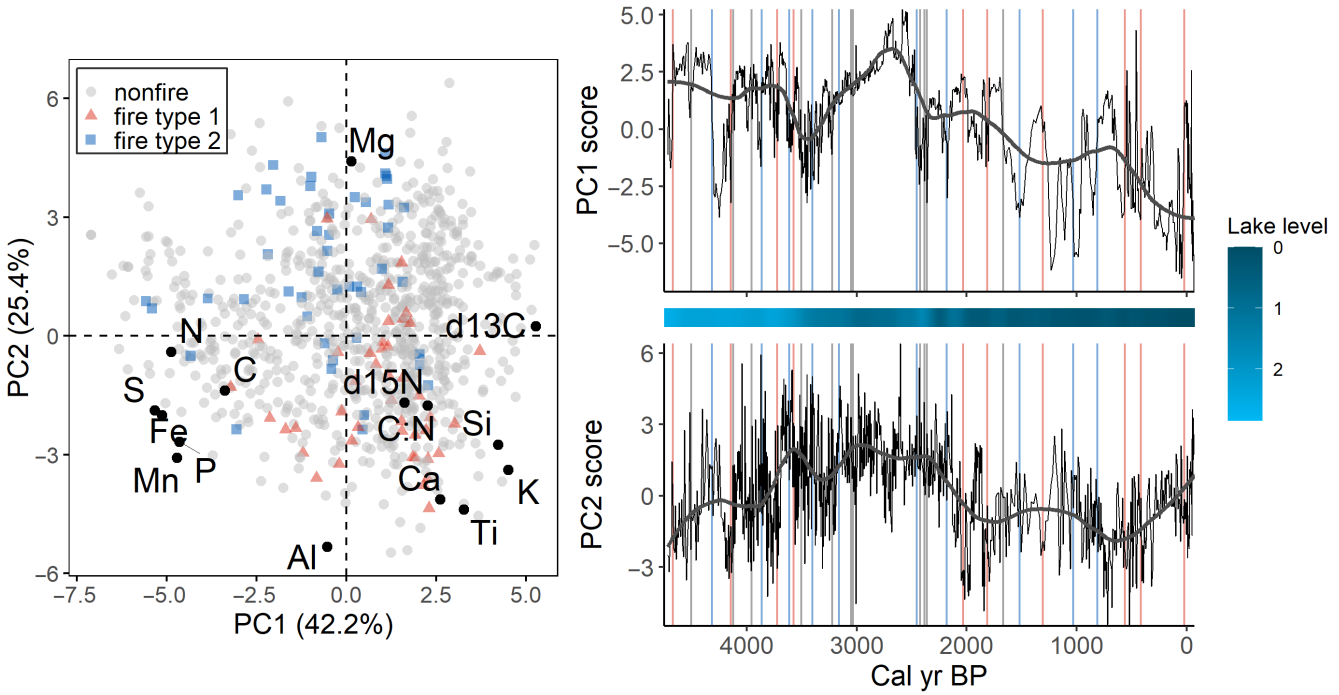

FIGURE 5 Principal components analysis summarizing variation in biogeochemical proxies. Left: biplot showing the location of each element and the axis scores of individual lake-sediment samples, which are displayed based on coincidence with charcoal-inferred fire events. Samples during or within 20 years following a biogeochemically impactful fire are shown in colour and nonfire samples are shown in grey. Right: time series displaying short-term variation (black line) and long-term trends (1000-year loess, thick grey line) in the first two principal components (PC1 and PC2), with vertical lines indicating the timing of inferred fire events. Red = Type 1 (erosion-associated) fires; blue = Type 2 (nonerosional) fires; grey = nonresponsive fires. The shaded bar shows variation in effective moisture at the site, represented using reconstructed lake-level anomalies in metres below modern, as in Figure 2, where darker colours indicate higher lake levels (i.e. greater effective moisture).

initial decrease in PC1 values and an increase in PC2 values relative to pre-fire. Additionally, there was weak to moderate evidence that nonerosional fires were followed by increases in average sediment C and S concentrations and decreases in Si ($p < 0.10$), although these responses and those in Al, K and Ca were not significant when medians were considered (Figure 6). All geochemical proxies returned to baseline values within c. 30–50-years postfire on average (Figure 6).

Pollen assemblages varied significantly based on time-since-fire (Figure 7). Fire effects on vegetation were most evident within 40 years after fire, and pollen assemblages typically returned to pre-fire values within c. 80 years after fire (Figure 7b). There was moderate evidence that conifer pollen abundance decreased and broadleaf pollen abundance increased initially after fire ($p < 0.05$), while AP:NAP and herbaceous pollen percentages did not change after fire (Figure 7a). Postfire changes in pollen abundances were, in large part, driven by initial decreases in percentages of *Pinus* and *Abies* pollen types and increases in percentages of *Alnus* pollen types and were broadly similar throughout the record. Changes in pollen assemblages were generally of higher magnitude following erosion-associated (Type 1) fires compared with nonerosional (Type 2) fires, but very small sample sizes limit our ability to interpret those differences (Figure S6).

4 | DISCUSSION

Consistent with our hypotheses, forests surrounding Silver Lake were sensitive to millennial-scale climatic changes, revealing a

FIGURE 6 Postfire responses of select geochemical proxies for Type 1 (erosion-associated, $n = 10$), Type 2 (nonerosional, $n = 10$) and nonresponsive ($n = 9$) fires, which were identified using hierarchical cluster analysis and screening for a postfire Ti response. Geochemical proxies are plotted as anomalies around the locally weighted mean. To show the range of postfire responses following individual fires, boxplots display values averaged over a baseline of 20–40 years before each fire and for 30-year time lags spanning 0–80 years following fire. P-values above plots give the result of Kruskal–Wallis tests, to evaluate the null hypothesis that the samples did not differ among lags before and after fire. To show the average response across fires, mean values for each time lag are displayed using points, with colours of postfire mean values denoting significant differences from the pre-fire mean (90%, 95% and 99% confidence based on 10,000 permutations).

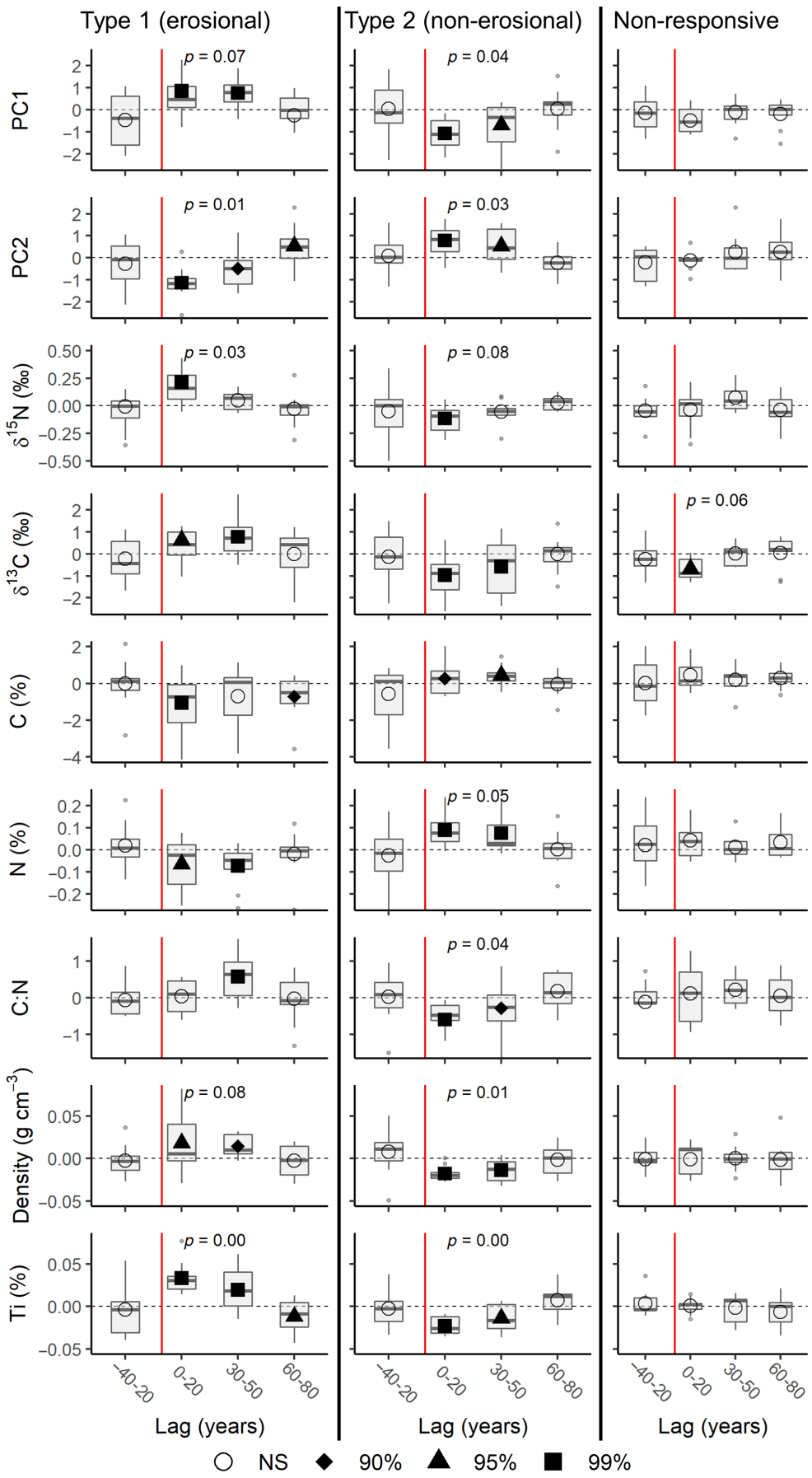

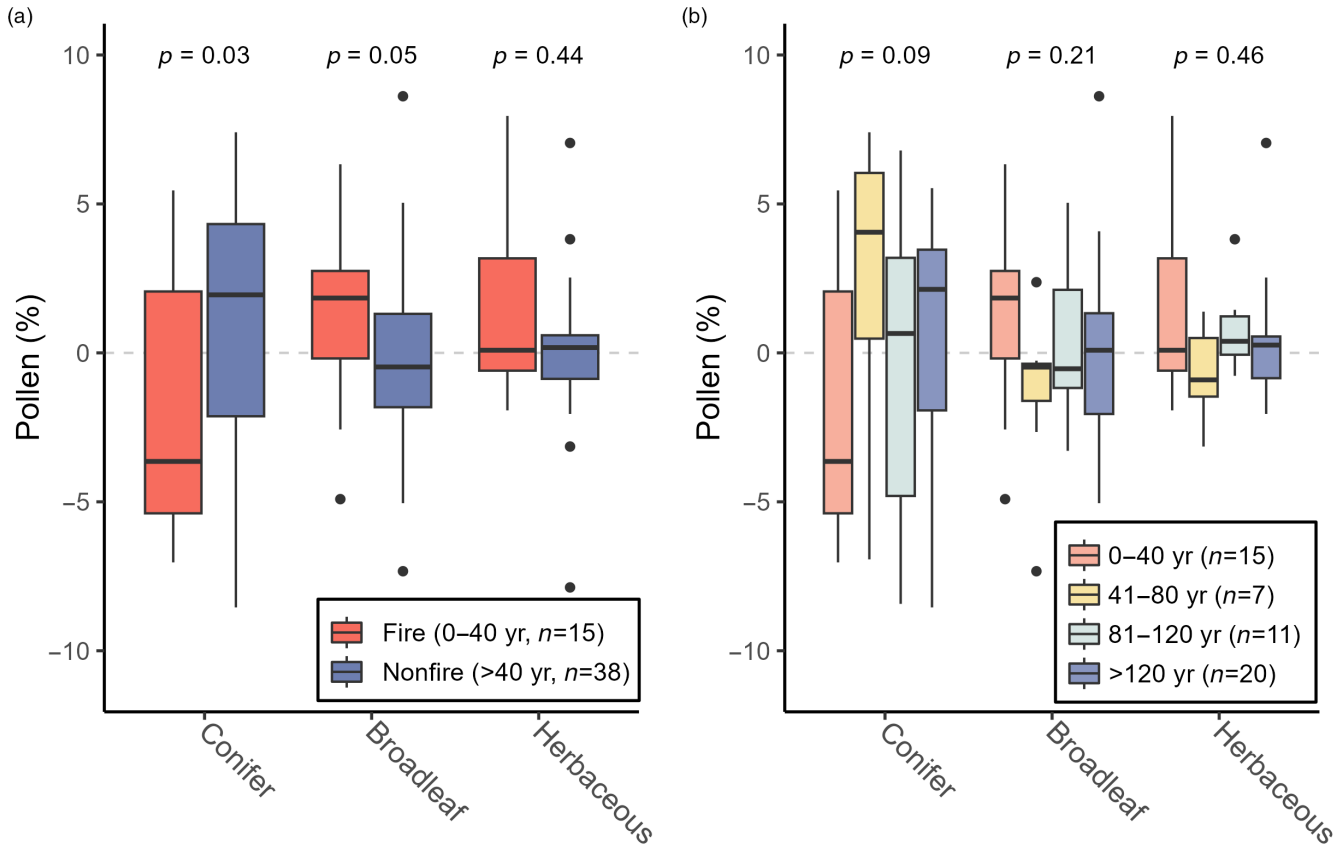

FIGURE 7 Boxplots comparing pollen abundance of major taxa among pollen samples with differing time-since-fire values, represented as anomalies from the locally weighted mean. (a) Grouped by time-since-fire, where fire-coincident ('fire') pollen samples are those from sediment samples within 0–40 years of a CHAR peak, and all other pollen samples are classed as 'nonfire'; (b) same as (a), with additional classifications for time-since-fire windows. *p*-values report the results of nonparametric Wilcoxon rank-sum tests (a) or Kruskal–Wallis tests (b). Major pollen taxa are summarized by dominant groups, as in Figure 4: Conifer (*Abies*, *Pinus*, *Picea*, *Tsuga mertensiana*, *Pseudotsuga-Larix*, Cupressaceae); Broadleaf (*Alnus rubra*, *Alnus viridis* ssp. *sinuata*); and Herbaceous (Poaceae, *Artemisia*, Asteroideae, *Ambrosia*, Ranunculaceae, Amaranthaceae).

long-term shift towards subalpine forest composition and decreased fire frequency, both likely attributable to greater effective moisture during the late Holocene. Ecosystem responses to individual fires were superimposed on these long-term trends. Contrary to our hypotheses, there was no evidence of shifting fire–ecosystem dynamics from millennial-scale climatic changes. Throughout repeated fire events over millennia, the forests surrounding Silver Lake demonstrated consistent biogeochemical resilience to wildfires, across variations in climate, fire frequency and fire effects. On decadal timescales, fire events had distinct and diverse biogeochemical effects throughout the sedimentary record. This characterization of past variation in fire severity provides a relatively rare example of heterogeneity in fire effects in the palaeorecord. Our study thus reveals decadal-to-millennial-scale fire–ecosystem relationships in temperate forests and provides a novel view into variability in past fire severity, which is recognized as a key challenge for understanding fire as a fundamental ecological process (McLauchlan et al., 2020).

4.1 | Millennial-scale context: Vegetation and fire regimes were sensitive to regional climatic changes

Millennial-scale trends in fire activity, vegetation and catchment biogeochemistry at Silver Lake underscore climate as an overarching control of ecosystem processes. These proxies also provide a long-term context in which we can examine decadal-scale ecosystem responses to individual fire events. Forest vegetation and fire frequency changed in response to a millennial-scale trend towards greater effective moisture, revealed by increasing lake level beginning c. 2800 yr BP and reaching near-modern levels c. 1800 yr BP (Figure 8). This shift in climate corresponded with an increase in pollen abundance of subalpine species and a 77% lengthening of the mFRI in the past two millennia (Figure 3). The estimated mFRI of 223 years (95% CI: 175–280 years; Table S2) for the past 1900 years aligns well with regional tree-ring and contemporary records from subalpine forests in the northern Rocky Mountains (mFRI estimates of 140–240 years; Gibson et al., 2014; Kipfmeuller, 2003). Decreased fire activity

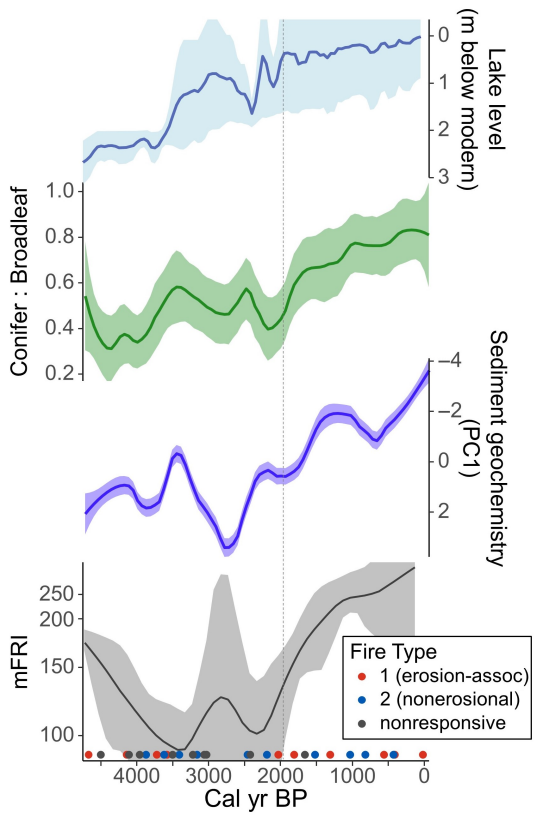

FIGURE 8 Fire, geochemical, vegetation and palaeoclimate history over the past 4800 years at Silver Lake. Millennial-scale trends in fire frequency are represented using a smoothed estimate of the mFRI. Points below the time series display the timing of charcoal peaks (red = Type 1, erosion-associated fires; blue = Type 2, nonerosional fires; grey = nonresponsive). Long-term variation in sediment geochemistry is summarized by PC1 values, and the vegetation history is represented by the ratio of major conifer-to-broadleaf pollen types, smoothed to show 1000-year trends with 95% confidence bands. Positive values of PC1 are associated with higher concentrations of minerogenic elements (see Figure 5). Palaeoclimate was inferred from a previously published lake-level reconstruction from Silver Lake (Parish et al., 2022). The vertical dotted line delineates the pollen zone break, which also corresponds to a significant change in fire frequency.

in the past two millennia is attributable to increased snowpack and later snowmelt from late Holocene climatic changes, which would favour higher summer fuel moisture and/or shorter fire seasons, consistent with contemporary fire–climate relationships in the region (Heyerdahl et al., 2008; Morgan et al., 2008; Westerling, 2016). Results from Silver Lake broadly align with existing palaeoecological records from the northern Rocky Mountains, which indicate the establishment of subalpine conifer forest c. 2000–4000 yr BP as a result of climatic cooling (e.g. Herring et al., 2017), and highlight strong links between climate and fire activity throughout the Holocene (e.g. Brunelle et al., 2005; Clark-Wolf, Higuera, Shuman, et al., 2023). Similar patterns of decreased fire frequency in recent millennia, associated with reduced summer insolation during the late Holocene, are also observed in other regions of North America (Girardin et al., 2013; Oris et al., 2014).

Millennial-scale climate change additionally exerted a strong influence on catchment biogeochemistry, independent of changing fire activity. The biogeochemical composition of Silver Lake sediments was broadly consistent with expected values for lacustrine sediments, providing integrated information about watershed processes such as terrestrial and aquatic productivity, N availability and soil erosion (Boyle, 2001; Meyers & Teranes, 2001; Appendix S2). The dominant millennial-scale trend in catchment biogeochemistry is characterized by the decline in PC1 over the past 2500 years (Figure 8), likely attributable to increased effective moisture and associated shifts in within-lake biogeochemical processes. Changes in the quantity or type of precipitation, as reflected in a higher lake level within the past 2000 years, would seem to increase the hydrological connections between the catchment and the lake at this site. It is also possible that changes in dust inputs could contribute to long-term variations in element concentrations (Aciego et al., 2017; Ballantyne et al., 2011).

4.2 | Decadal-scale fire–ecosystem interactions

Multiple distinct biogeochemical effects of past wildfires are well-resolved in the Silver Lake record, revealing diversity in fire effects rarely discernible in palaeofire records. Sediment biogeochemistry changed distinctly in response to fire events, representing varying fire effects related to fire behaviour and severity (i.e. direct, or first-order fire effects), as well as ecosystem dynamics over successional timescales after fire (i.e. indirect, or second-order fire effects). Given the decadal-scale resolution of the record, we cannot distinguish between direct and indirect fire effects. Nonetheless, we frame our discussion in the context of inferred fire severity and subsequent biogeochemical responses over successional timescales.

Nearly half of fire events reconstructed ($n = 10$) had biogeochemical responses consistent with an influx of material from postfire soil erosion; these events were likely spatially extensive, high-severity fires that burned in the watershed. We interpret initial increases in the concentrations of Ti and other lithogenic elements as evidence of fire-related erosion, which is also associated with elevated sediment bulk density reflecting an influx of clastic detritus (Figure 6), similar to the biogeochemical impacts of lake-sediment-inferred high-severity fires in a subalpine watershed in Colorado (Dunnette et al., 2014; Leys et al., 2016). Intense and spatially continuous burning enhances erosion via reduced interception and increased soil water repellency, resulting in greater overland flows and a redistribution of topsoil and associated elements within the watershed (Berhe et al., 2018; Larsen et al., 2009; Shakesby & Doerr, 2006; Vieira et al., 2015). Additionally, postfire increases in sedimentary $\delta^{15}N$ values are consistent with a more 'open' N cycle initially following fire (Dunnette et al., 2014; LeDuc et al., 2013; Perakis et al., 2015). High-severity wildfires can increase the $\delta^{15}N$ of terrestrial N via preferential volatilization of the lighter isotope, combustion of isotopically depleted foliar and litter N

pools, as well as elevated nitrification and nitrate leaching after fire, given that nitrification strongly discriminates against the heavier isotope (Hoberg, 1997). In turn, changes in the size and isotopic makeup of terrestrial N pools alter the N budget and sedimentary $\delta^{15}N$ values of closely linked lacustrine systems (Dunnette et al., 2014; Hu et al., 2001; Kim et al., 2016; Morris et al., 2015).

An equal number of fire events ($n = 10$) was associated with increased organic inputs and nutrient subsidies to the lake, lacking any indications of fire-caused soil erosion (Figure 6). We interpret these nonerosional fire events as non-stand-replacing fires or high-severity fires that burned a lesser proportion of the catchment. Importantly, these events were still impactful enough to influence biogeochemical processes. For example, soil inorganic nitrogen pools often increase dramatically over months to years postfire (Smithwick et al., 2005; Wan et al., 2001), and nutrients delivered to lakes via riverine and subsurface flows following fires (e.g. Gustine et al., 2022; Rhoades et al., 2011; Spencer et al., 2003) may stimulate within-lake algal production, as implied by low sediment C:N and bulk density postfire (McCullough et al., 2019; Morris & Lewis, 1988; Figure 6). Indeed, elevated lake-sediment N 0–20 years after palaeofires at Gold Creek Lake, Colorado, was interpreted as evidence of increased aquatic productivity (Pompeani et al., 2020), a pattern also evident in Silver Lake (Figure 6). Postfire changes in N cycling over decadal timescales could also be related to fire-produced charcoal, which can increase soil nitrification potential (DeLuca & Sala, 2006). Low $\delta^{15}N$ values indicate strong recovery of N conservation following these non-stand-replacing fires, through either microbial immobilization or plant uptake (e.g. Turner et al., 2007). Additionally, growth of symbiotic and nonsymbiotic N fixers following fire (e.g. *Alnus*, Figure 7) could lower the $\delta^{15}N$ of terrestrial N pools, highlighting biotic controls on catchment biogeochemistry (Cleveland et al., 2022; Perakis et al., 2015; Yelenik et al., 2013). Importantly, these results reveal that differences in fire severity can lead to divergent responses in N-cycle dynamics over decadal timescales, such that the biogeochemical implications of a fire-regime shift would depend on changes in both fire frequency and severity.

Finally, nearly an equal proportion of fire events ($n = 9$) was associated with a lack of significant biogeochemical responses. We interpret these as reflecting lower-severity, spatially variable fires within the watershed, or fires burning nearby but outside of the watershed (e.g. 1–2 km). Evidence of changes in pollen assemblages following these fire events indicates that they indeed represent burning within the pollen and charcoal source areas of Silver Lake (Figure S6). The only distinct change in biogeochemical proxies after these fires was an initial decrease in $\delta^{13}C$ (Figure 6), which may simply reflect the influx of charcoal itself, given that partial combustion can deplete wood $\delta^{13}C$ by up to 1.6‰ (Ascough et al., 2008).

4.3 | Ecosystem resilience to wildfires

Our results highlight consistent ecosystem resilience to wildfires throughout the past 4800 years, despite variations in climate, vegetation and fire activity (Figure 8). Regardless of the type of postfire response, biogeochemical proxies and pollen assemblages recovered to pre-fire values within c. 50–80 years (Figures 6 and 7), consistent with expectations that re-establishment of vegetation would stabilize soils, and forest aggradation would conserve nitrogen through increased plant uptake demand (Cerdà et al., 2005; Kim et al., 2016, 2021; Turner et al., 2007). Average recovery times were less than the average FRI, revealing consistent ecosystem resilience to fire. Evidence of ecosystem resilience to palaeofires at Silver Lake also aligns with several records from subalpine and boreal forest sites (Carcaillet et al., 2020; Chipman & Hu, 2019; Dunnette et al., 2014; Pompeani et al., 2020) and highlights tight linkages between vegetation and biogeochemical processes over successional timescales (Smithwick, 2011). Additionally, a diversity of fire effects was evident throughout the record, providing support for ecosystem resilience to a variety of disturbance processes. Thus, although the ecosystem experienced millennial-scale changes in climate and vegetation over the late Holocene, it retained the ability to return to predisturbance vegetation and biogeochemical states within decades following individual fires. As such, we did not observe a 'stair step' response of directional trends in nutrient availability over multiple disturbance intervals (McLauchlan et al., 2014); rather, low millennial-scale variation in sediment $\delta^{15}N$ indicates that overall ecosystem nitrogen availability remained fairly stable despite postfire fluctuations (e.g. Kim et al., 2016; Robinson, 2001).

The varying direction and magnitude of decadal-scale biogeochemical changes following fire events provide an example of variability in the characteristics and effects of individual fires, reflecting differences in fire behaviour (e.g. intensity and duration) and severity. Large and severe wildfires caused a loss of N and base cations from the terrestrial environment (e.g. Bormann et al., 2008), whereas shifts in nutrient cycling were evident following lower-severity or patchier fires lacking significant soil erosion. Similar changes could also occur following severe fires, but may be diluted or obscured by eroded material, such that the dominant processes preserved in lake sediments differ among fires. Our results thus underscore the importance of fire behaviour and the resulting severity as key controls of fire effects on the amounts and fluxes of C and other elements (Adkins et al., 2019; Li et al., 2021; Raison, 1979; Smithwick et al., 2005). Importantly, this diversity in fire effects occurred throughout the past 4800 years at Silver Lake, within multi-millennial periods characterized by the same general climate and vegetation conditions, as well as inferred fire regime (Figure 8). This pattern is contrary to our original hypothesis, indicating that a shift towards cooler climate and lower fire frequency in the past two millennia did not lead to a directional shift in fire–ecosystem relationships through changes in fire severity or recovery time. Thus, decadal-scale ecosystem responses to fire can exhibit complacency despite fire-regime shifts, and the ecosystem impacts of individual fires are heterogeneous even within a single site. Our work highlights that this heterogeneity has been the case for millennia, thus characterizing historical variability in multiple components of past fire regimes.

The diversity of fire severity and fire effects revealed over the past 4800 years is analogous to spatial variability in fire severity observed within contemporary wildfires. Approximately one third of fire events identified in the Silver Lake record fell into the categories of erosion-associated, nonerosional or nonresponsive, likely reflecting differences in fuels, fire weather and fire behaviour (e.g. Evers et al., 2022). Within contemporary forest fires in the northern Rocky Mountains (all elevations), 34% of forest fire area over 1984–2010 burned at high severity, with the remainder burning at moderate or low severity (Harvey et al., 2016). Thus, even in forest types characterized by infrequent high-severity fire regimes—where many fires kill nearly 100% of trees—patches of non-stand-replacing fire contribute to spatial and temporal complexity in forest structure and species composition. Such complexity is hypothesized to support biodiversity (Jones & Tingley, 2022; Martin & Sapsis, 1992), and although we cannot test that hypothesis with the data presented here, future research bringing together palaeoenvironmental records from multiple sites would provide greater statistical power for evaluating how variation in fire timing and severity influences ecosystem dynamics.

4.4 | Implications for future ecosystem change

The overarching influence of climate on disturbance and ecosystem processes across the Silver Lake record implies that ongoing and future climate change will likewise impact disturbance and ecosystem processes. Fire activity in the study region is projected to nearly double by the late 21st century under high emissions scenarios as a result of increased atmospheric aridity, relative to a 1979–2000 baseline (Gao et al., 2021). The higher-than-present fire frequency observed at Silver Lake between 4800 and 1900 yr BP provides an imperfect analogue for ecological dynamics with more frequent fire. Our results suggest that ecosystem resilience could be maintained, if fire-free periods at the forest stand level remain on average greater than our estimated biogeochemical recovery time of c. 50–80 years. However, warmer and drier conditions or more severe fires relative to the past four millennia could increase the time needed to recover, or alter postfire ecological trajectories, undermining the long-standing ecosystem resilience revealed in the palaeorecord (Johnstone et al., 2016; McLauchlan et al., 2014; Turner et al., 2019).

Feedbacks between shifting fire activity and ecosystem changes may also emerge. Our results indicate that non-stand-replacing fires have been an important component of the fire regime for millennia around Silver Lake, including during a period of drier conditions characterized by more frequent burning and likely lower forest density c. 4800–1900 yr BP (Figure 8). With ongoing climate change, increasing area burned and shifts in forest composition or structure could lead to feedbacks whereby fuel types or availability mitigate fire severity and C emissions (Mack et al., 2021; Parks et al., 2016; Walker et al., 2020). As such, a range of fire severities and biogeochemical impacts could be supported even under warmer and drier climate conditions. Such feedbacks are unlikely to manifest in the next several decades (Abatzoglou et al., 2021), but could ultimately promote forest resilience over centennial timescales. Still, it remains unclear when, where and how ecosystem transformations will unfold under rapid climate change (Anderson-Teixeira et al., 2013; Seidl & Turner, 2022). Clarifying feedbacks among fire regimes, vegetation and forest biogeochemistry is clearly needed to help anticipate the impacts of ongoing warming and inform management agendas (Crausbay et al., 2022).

AUTHOR CONTRIBUTIONS

Kyra Clark-Wolf, Philip Higuera, Kendra McLauchlan and Bryan Shuman conceived the ideas and designed methodology; Kyra Clark-Wolf collected novel data and Meredith Parish contributed data; Kyra Clark-Wolf analysed the data; Kyra Clark-Wolf and Philip Higuera led the writing of the manuscript. All authors contributed critically to the drafts and gave final approval for publication.

ACKNOWLEDGEMENTS

We thank the Big Burns team, including K. Bartowitz, T. Hudiburg, D. Pompeani and B. Chileen for their long-standing contributions to the project. We thank A. Young and K. Davis for assistance with field sample collection, E. Herring for data sharing and pollen analyses and J. Roozeboom and D. Darter for XRF analyses. We thank L. Converse, L. Crofutt, A. Hendryx, K. Mooney, M. Miller and I. Evavold for their diligent work on sediment processing and charcoal sieving. This project was supported by NSF award DEB-1655121 to PEH, DEB-1655179 to KKM and DEB-1655189 to BNS.

CONFLICT OF INTEREST STATEMENT

The authors declare no conflicts of interest associated with this publication.

DATA AVAILABILITY STATEMENT

Data and code associated with this manuscript are publicly available via Dryad Digital Repository https://doi.org/10.5061/dryad.x0k6djhpr (Clark-Wolf, Higuera, McLauchlan, et al., 2023).

ORCID

Kyra D. Clark-Wolf https://orcid.org/0000-0003-4584-0348
Philip E. Higuera https://orcid.org/0000-0001-5396-9956
Kendra K. McLauchlan https://orcid.org/0000-0002-6612-1097
Bryan N. Shuman https://orcid.org/0000-0002-8149-8925
Meredith C. Parish https://orcid.org/0000-0001-7159-3358

REFERENCES

Abatzoglou, J. T., Battisti, D. S., Williams, A. P., Hansen, W. D., Harvey, B. J., & Kolden, C. A. (2021). Projected increases in western US forest fire despite growing fuel constraints. *Communications Earth & Environment*, *2*(1), 1–8. https://doi.org/10.1038/s43247-021-00299-0

Abatzoglou, J. T., & Williams, A. P. (2016). Impact of anthropogenic climate change on wildfire across western US forests. *Proceedings of the National Academy of Sciences of the United States of America*, *113*(42), 11770–11775. https://doi.org/10.1073/pnas.1607171113

Aciego, S. M., Riebe, C. S., Hart, S. C., Blakowski, M. A., Carey, C. J., Aarons, S. M., Dove, N. C., Botthoff, J. K., Sims, K. W. W., & Aronson,

E. L. (2017). Dust outpaces bedrock in nutrient supply to montane forest ecosystems. *Nature Communications*, *8*(1), Article 1. https://doi.org/10.1038/ncomms14800

Adkins, J., Sanderman, J., & Miesel, J. (2019). Soil carbon pools and fluxes vary across a burn severity gradient three years after wildfire in Sierra Nevada mixed-conifer forest. *Geoderma*, *333*, 10–22. https://doi.org/10.1016/J.GEODERMA.2018.07.009

Anderson-Teixeira, K. J., Miller, A. D., Mohan, J. E., Hudiburg, T. W., Duval, B. D., & DeLucia, E. H. (2013). Altered dynamics of forest recovery under a changing climate. *Global Change Biology*, *19*(7), 2001–2021. https://doi.org/10.1111/gcb.12194

Ascough, P. L., Bird, M. I., Wormald, P., Snape, C. E., & Apperley, D. (2008). Influence of production variables and starting material on charcoal stable isotopic and molecular characteristics. *Geochimica et Cosmochimica Acta*, *72*(24), 6090–6102. https://doi.org/10.1016/j.gca.2008.10.009

Bailey, R. G. (1995). Descriptions of the ecoregions of the United States: US Department of Agriculture. *Forest Service*, *Miscellaneous Publication*, *1391*, 108.

Ballantyne, A. P., Brahney, J., Fernandez, D., Lawrence, C. L., Saros, J., & Neff, J. C. (2011). Biogeochemical response of alpine lakes to a recent increase in dust deposition in the southwestern, US. *Biogeosciences*, *8*(9), 2689–2706. https://doi.org/10.5194/bg-8-2689-2011

Berhe, A. A., Barnes, R. T., Six, J., & Marín-Spiotta, E. (2018). Role of soil erosion in biogeochemical cycling of essential elements: Carbon, nitrogen, and phosphorus. *The Annual Review of Earth and Planetary Sciences*, *46*, 521–569. https://doi.org/10.1146/annurev-earth-082517

Binford, M. W. (1990). Calculation and uncertainty analysis of 210Pb dates for PIRLA project lake sediment cores. *Journal of Paleolimnology*, *3*(3), 253–267. https://doi.org/10.1007/bf00219461

Blaauw, M., & Christen, J. A. (2011). Flexible paleoclimate age-depth models using an autoregressive gamma process. *Bayesian Analysis*, *6*(3), 457–474. https://doi.org/10.1214/11-BA618

Blarquez, O., & Carcaillet, C. (2010). Fire, fuel composition and resilience threshold in subalpine ecosystem. *PLoS ONE*, *5*(8), e12480. https://doi.org/10.1371/journal.pone.0012480

Bormann, B. T., Homann, P. S., Darbyshire, R. L., & Morrissette, B. A. (2008). Intense forest wildfire sharply reduces mineral soil C and N: The first direct evidence. *Canadian Journal of Forest Research*, *38*(11), 2771–2783. https://doi.org/10.1139/X08-136

Bowd, E. J., Lindenmayer, D. B., Banks, S. C., & Blair, D. P. (2018). Logging and fire regimes alter plant communities. *Ecological Applications*, *28*(3), 826–841. https://doi.org/10.1002/eap.1693

Boyle, J. (2001). Inorganic geochemical methods in paleolimnology. In *Tracking environmental change using Lake sediments: Physical and geochemical methods* (Vol. *2*, 1st ed., pp. 83–141). Kulwer Academic Publishers.

Brenner, M., Whitmore, T. J., Curtis, J. H., Hodell, D. A., & Schelske, C. L. (1999). Stable isotope (δ^{13}C and δ^{15}N) signatures of sedimented organic matter as indicators of historic lake trophic state. *Journal of Paleolimnology*, *22*(2), 205–221. https://doi.org/10.1023/A:1008078222806

Brunelle, A., Whitlock, C., Bartlein, P., & Kipfmueller, K. (2005). Holocene fire and vegetation along environmental gradients in the northern Rocky Mountains. *Quaternary Science Reviews*, *24*(20), 2281–2300. https://doi.org/10.1016/j.quascirev.2004.11.010

Carcaillet, C., Desponts, M., Robin, V., & Bergeron, Y. (2020). Long-term steady-state dry boreal forest in the face of disturbance. *Ecosystems*, *23*(5), 1075–1092. https://doi.org/10.1007/s10021-019-00455-w

Carcaillet, C., Richard, P. J. H., Bergeron, Y., Fréchette, B., Ali, A. A., Carcaillet, C., Richard, P. J. H., Bergeron, Y., Fréchette, B., & Ali, A. A. (2010). Resilience of the boreal forest in response to Holocene fire-frequency changes assessed by pollen diversity and population dynamics. *International Journal of Wildland Fire*, *19*(8), 1026–1039. https://doi.org/10.1071/WF09097

Cerdà, A., Doerr, S. H., Cerdà, A., & Doerr, S. H. (2005). Influence of vegetation recovery on soil hydrology and erodibility following fire: An 11-year investigation. *International Journal of Wildland Fire*, *14*(4), 423–437. https://doi.org/10.1071/WF05044

Chen, G., Hayes, D. J., David McGuire, A., & McGuire, A. D. (2017). Contributions of wildland fire to terrestrial ecosystem carbon dynamics in North America from 1990 to 2012. *Global Biogeochemical Cycles*, *31*(5), 878–900. https://doi.org/10.1002/2016GB005548

Chileen, B. V., McLauchlan, K. K., Higuera, P. E., Parish, M., & Shuman, B. N. (2020). Vegetation response to wildfire and climate forcing in a Rocky Mountain lodgepole pine forest over the past 2500 years. *The Holocene*, *30*(11), 1493–1503. https://doi.org/10.1177/0959683620941068

Chipman, M. L., & Hu, F. S. (2019). Resilience of lake biogeochemistry to boreal-forest wildfires during the late Holocene. *Biology Letters*, *15*(8), 20190390. https://doi.org/10.1098/rsbl.2019.0390

Clark-Wolf, K., Higuera, P., McLauchlan, K. K., Shuman, B., & Parish, M. (2023). Data archive for: Fire-regime variability and ecosystem resilience over four millennia in a Rocky Mountain subalpine watershed [Dataset]. *Dryad Digital Repository*, https://doi.org/10.5061/dryad.x0k6djhpr

Clark-Wolf, K., Higuera, P. E., Shuman, B. N., & McLauchlan, K. K. (2023). Wildfire activity in northern Rocky Mountain subalpine forests still within millennial-scale range of variability. *Environmental Research Letters*, *18*, 094029. https://doi.org/10.1088/1748-9326/acee16

Cleveland, C. C., Reis, C. R. G., Perakis, S. S., Dynarski, K. A., Batterman, S. A., Crews, T. E., Gei, M., Gundale, M. J., Menge, D. N. L., Peoples, M. B., Reed, S. C., Salmon, V. G., Soper, F. M., Taylor, B. N., Turner, M. G., & Wurzburger, N. (2022). Exploring the role of cryptic nitrogen fixers in terrestrial ecosystems: A frontier in nitrogen cycling research. *Ecosystems*, *25*, 1653–1669. https://doi.org/10.1007/s10021-022-00804-2

Cleveland, W. S. (1979). Robust locally weighted regression and smoothing scatterplots. *Journal of the American Statistical Association*, *74*(368), 829–836. https://doi.org/10.1080/01621459.1979.10481038

Coop, J. D., Parks, S. A., Stevens-Rumann, C. S., Crausbay, S. D., Higuera, P. E., Hurteau, M. D., Tepley, A., Whitman, E., Assal, T., Collins, B. M., Davis, K. T., Dobrowski, S., Falk, D. A., Fornwalt, P. J., Fulé, P. Z., Harvey, B. J., Kane, V. R., Littlefield, C. E., Margolis, E. Q., … Rodman, K. C. (2020). Wildfire-driven Forest conversion in Western north American landscapes. *BioScience*, *70*(8), 659–673. https://doi.org/10.1093/biosci/biaa061

Crausbay, S. D., Sofaer, H. R., Cravens, A. E., Chaffin, B. C., Clifford, K. R., Gross, J. E., Knapp, C. N., Lawrence, D. J., Magness, D. R., Miller-Rushing, A. J., Schuurman, G. W., & Stevens-Rumann, C. S. (2022). A science agenda to inform natural resource management decisions in an era of ecological transformation. *BioScience*, *72*(1), 71–90. https://doi.org/10.1093/biosci/biab102

Davies, S. J., Lamb, H. F., & Roberts, S. J. (2015). Micro-XRF core scanning in palaeolimnology: Recent developments. In I. W. Croudace & R. G. Rothwell (Eds.), *Micro-XRF studies of sediment cores: Applications of a non-destructive tool for the environmental sciences* (pp. 189–226). Springer Netherlands. https://doi.org/10.1007/978-94-017-9849-5_7

DeLuca, T. H., & Sala, A. (2006). Frequent fire alters nitrogen transformation in ponderosa pine stands of the Island northwest. *Ecology*, *87*(10), 2511–2522. https://doi.org/10.1890/0012-9658(2006)87[2511:FFANTI]2.0.CO;2

Dombrosky, J. (2020). A ~1000-year ^{13}C Suess correction model for the study of past ecosystems. *The Holocene*, *30*(3), 474–478. https://doi.org/10.1177/0959683619887416

Dove, N. C., Safford, H. D., Bohlman, G. N., Estes, B. L., & Hart, S. C. (2020). High-severity wildfire leads to multi-decadal impacts on soil biogeochemistry in mixed-conifer forests. *Ecological Applications*, *30*, e02072. https://doi.org/10.1002/eap.2072

Dray, S., & Dufour, A.-B. (2007). The ade4 package: Implementing the duality diagram for ecologists. *Journal of Statistical Software*, *22*(4), 20. https://doi.org/10.18637/jss.v022.i04

Dunnette, P. V., Higuera, P. E., McLauchlan, K. K., Derr, K. M., Briles, C. E., & Keefe, M. H. (2014). Biogeochemical impacts of wildfires over four millennia in a Rocky Mountain subalpine watershed. *New Phytologist*, *203*(3), 900–912. https://doi.org/10.1111/nph.12828

Egan, J., Staff, R., & Blackford, J. (2015). A high-precision age estimate of the Holocene Plinian eruption of mount mazama, Oregon, USA. *The Holocene*, *25*(7), 1054–1067. https://doi.org/10.1177/0959683615576230

Evers, C., Holz, A., Busby, S., & Nielsen-Pincus, M. (2022). Extreme winds alter influence of fuels and topography on megafire burn severity in seasonal temperate rainforests under record fuel aridity. *Fire*, *5*(2), Article 2. https://doi.org/10.3390/fire5020041

Fægri, K., Kaland, P. E., & Krzywinski, K. (1989). *Textbook of pollen analysis* (4th ed.). https://www.cabdirect.org/cabdirect/abstract/19930670810

Falk, D. A., van Mantgem, P. J., Keeley, J. E., Gregg, R. M., Guiterman, C. H., Tepley, A. J., Young, D. J. N., & Marshall, L. A. (2022). Mechanisms of forest resilience. *Forest Ecology and Management*, *512*, 120129. https://doi.org/10.1016/j.foreco.2022.120129

Gao, P., Terando, A. J., Kupfer, J. A., Morgan Varner, J., Stambaugh, M. C., Lei, T. L., & Kevin Hiers, J. (2021). Robust projections of future fire probability for the conterminous United States. *Science of the Total Environment*, *789*, 147872. https://doi.org/10.1016/j.scitotenv.2021.147872

Genries, A., Mercier, L., Lavoie, M., Muller, S. D., Radakovitch, O., & Carcaillet, C. (2009). The effect of fire frequency on local cembra pine populations. *Ecology*, *90*(2), 476–486. https://doi.org/10.1890/07-1740.1

Gibson, C. E., Morgan, P., & Wilson, A. M. (2014). *Atlas of digital polygon fire extents for Idaho and western Montana* [dataset] (2nd ed.). Forest Service Research Data Archive. https://doi.org/10.2737/RDS-2009-0006-2

Girardin, M. P., Ali, A. A., Carcaillet, C., Blarquez, O., Hély, C., Terrier, A., Genries, A., & Bergeron, Y. (2013). Vegetation limits the impact of a warm climate on boreal wildfires. *New Phytologist*, *199*(4), 1001–1011. https://doi.org/10.1111/nph.12322

Gunderson, L. H. (2000). Ecological resilience—In theory and application. *Annual Review of Ecology and Systematics*, *31*(1), 425–439. https://doi.org/10.1146/annurev.ecolsys.31.1.425

Gustine, R. N., Hanan, E. J., Robichaud, P. R., & Elliot, W. J. (2022). From burned slopes to streams: How wildfire affects nitrogen cycling and retention in forests and fire-prone watersheds. *Biogeochemistry*, *157*(1), 51–68. https://doi.org/10.1007/s10533-021-00861-0

Hart, S. C., DeLuca, T. H., Newman, G. S., MacKenzie, M. D., & Boyle, S. I. (2005). Post-fire vegetative dynamics as drivers of microbial community structure and function in forest soils. *Forest Ecology and Management*, *220*(1), 166–184. https://doi.org/10.1016/j.foreco.2005.08.012

Harvey, B. J., Donato, D. C., & Turner, M. G. (2016). Drivers and trends in landscape patterns of stand-replacing fire in forests of the US Northern Rocky Mountains (1984–2010). *Landscape Ecology*, *31*, 2367–2383. https://doi.org/10.1007/s10980-016-0408-4

Herring, E. M., Gavin, D. G., Dobrowski, S. Z., Fernandez, M., & Hu, F. S. (2017). Ecological history of a long-lived conifer in a disjunct population. *Journal of Ecology*, *106*(1), 319–332. https://doi.org/10.1111/1365-2745.12826

Heyerdahl, E. K., Morgan, P., & Riser, J. P. (2008). Multi-season climate synchronized historical fires in dry forests (1650–1900) northern Rockies, USA. *Ecology*, *89*(3), 705–716. https://doi.org/10.1890/06-2047.1

Higuera, P. (2009). *CharAnalysis 0.9: Diagnostic and analytical tools for sedimentcharcoal analysis*. User's Guide. https://github.com/phiguera/CharAnalysis

Higuera, P. E., Brubaker, L. B., Anderson, P. M., Hu, F. S., & Brown, T. A. (2009). Vegetation mediated the impacts of postglacial climate change on fire regimes in the south-central Brooks Range, Alaska. *Ecological Monographs*, *79*(2), 201–219. https://doi.org/10.1890/07-2019.1

Hoberg, P. (1997). Tansley review no. 95 ^{15}N natural abundance in soil-plant systems. *New Phytologist*, *137*(2), 179–203. https://doi.org/10.1046/j.1469-8137.1997.00808.x

Hu, F. S., Finney, B. P., & Brubaker, L. B. (2001). Effects of holocene alnus expansion on aquatic productivity, nitrogen cycling, and soil development in southwestern Alaska. *Ecosystems*, *4*(4), 358–368. https://doi.org/10.1007/s10021-001-0017-0

Hudiburg, T. W., Higuera, P. E., & Hicke, J. A. (2017). Fire-regime variability impacts forest carbon dynamics for centuries to millennia. *Biogeosciences*, *14*(17), 3873–3882. https://doi.org/10.5194/bg-14-3873-2017

Jiménez-Moreno, G., Anderson, R. S., Atudorei, V., & Toney, J. L. (2011). A high-resolution record of climate, vegetation, and fire in the mixed conifer forest of northern Colorado, USA. *GSA Bulletin*, *123*(1–2), 240–254. https://doi.org/10.1130/B30240.1

Johnson, E. A., & Gutsell, S. L. (1994). Fire frequency models, methods and interpretations. *Advances in Ecological Research*, *25*, 239–287.

Johnstone, J. F., Allen, C. D., Franklin, J. F., Frelich, L. E., Harvey, B. J., Higuera, P. E., Mack, M. C., Meentemeyer, R. K., Metz, M. R., Perry, G. L. W., Schoennagel, T., & Turner, M. G. (2016). Changing disturbance regimes, ecological memory, and forest resilience. *Frontiers in Ecology and the Environment*, *14*(7), 369–378. https://doi.org/10.1002/fee.1311

Jones, G. M., & Tingley, M. W. (2022). Pyrodiversity and biodiversity: A history, synthesis, and outlook. *Diversity and Distributions*, *28*(3), 386–403. https://doi.org/10.1111/ddi.13280

Kapp, R. O., Davis, O. K., & King, J. E. (2000). *Guide to pollen and spores* (2nd ed.). American Association of Stratigraphic Palynologists Foundation.

Kelly, R., Genet, H., McGuire, A. D., & Hu, F. S. (2015). Palaeodata-informed modelling of large carbon losses from recent burning of boreal forests. *Nature Climate Change*, *6*(1), 79. https://doi.org/10.1038/nclimate2832

Kelly, R. F., Higuera, P. E., Barrett, C. M., & Hu, F. S. (2011). A signal-to-noise index to quantify the potential for peak detection in sediment–charcoal records. *Quaternary Research*, *75*(1), 11–17. https://doi.org/10.1016/j.yqres.2010.07.011

Kim, S. L., Shuman, B. N., Minckley, T. A., & Marsicek, J. P. (2016). Biogeochemical change during climate-driven afforestation: A paleoecological perspective from the Rocky Mountains. *Ecosystems*, *19*(4), 615–624. https://doi.org/10.1007/s10021-015-9955-9

Kim, Y., Kim, C.-G., Lee, K. S., & Choung, Y. (2021). Effects of post-fire vegetation recovery on soil erosion in vulnerable montane regions in a monsoon climate: A decade of monitoring. *Journal Of Plant Biology*, *64*(2), 123–133. https://doi.org/10.1007/s12374-020-09283-1

Kipfmeuller, K. F. (2003). *Fire-climate-vegetation interactions in subalpine forests of the Selway-Bitterroot Wilderness Area, Idaho and Montana, United States*. The University of Arizona. http://hdl.handle.net/10150/280300

Kirchmeier-Young, M. C., Zwiers, F. W., Gillett, N. P., & Cannon, A. J. (2017). Attributing extreme fire risk in Western Canada to human emissions. *Climatic Change*, *144*(2), 365–379. https://doi.org/10.1007/s10584-017-2030-0

Larsen, I. J., MacDonald, L. H., Brown, E., Rough, D., Welsh, M. J., Pietraszek, J. H., Libohova, Z., de Dios Benavides-Solorio, J., & Schaffrath, K. (2009). Causes of post-fire runoff and erosion: Water repellency, cover, or soil sealing? *Soil Science Society of America Journal*, *73*(4), 1393–1407. https://doi.org/10.2136/sssaj2007.0432

LeDuc, S. D., Rothstein, D. E., Yermakov, Z., & Spaulding, S. E. (2013). Jack pine foliar δ^{15}N indicates shifts in plant nitrogen acquisition after severe wildfire and through forest stand development. *Plant and Soil*, *373*(1–2), 955–965. https://doi.org/10.1007/s11104-013-1856-0

Leys, B. A., Higuera, P. E., McLauchlan, K. K., & Dunnette, P. V. (2016). Wildfires and geochemical change in a subalpine forest over the past six millennia. *Environmental Research Letters*, *11*(12), 125003. https://doi.org/10.1088/1748-9326/11/12/125003

Li, J., Pei, J., Liu, J., Wu, J., Li, B., Fang, C., & Nie, M. (2021). Spatiotemporal variability of fire effects on soil carbon and nitrogen: A global meta-analysis. *Global Change Biology*, *27*(17), 4196–4206. https://doi.org/10.1111/gcb.15742

Mack, M. C., Walker, X. J., Johnstone, J. F., Alexander, H. D., Melvin, A. M., Jean, M., & Miller, S. N. (2021). Carbon loss from boreal forest wildfires offset by increased dominance of deciduous trees. *Science*, *372*(6539), 280–283. https://doi.org/10.1126/science.abf3903

Martin, R., & Sapsis, D. (1992). *Fires as agents of biodiversity: Pyrodiversity promotes biodiversity*. Proceedings of the conference on biodiversity of Northwest California ecosystems, cooperative extension, University of California, Berkeley.

McCullough, I. M., Cheruvelil, K. S., Lapierre, J., Lottig, N. R., Moritz, M. A., Stachelek, J., & Soranno, P. A. (2019). Do lakes feel the burn? Ecological consequences of increasing exposure of lakes to fire in the continental United States. *Global Change Biology*, *25*(9), 2841–2854. https://doi.org/10.1111/gcb.14732

McLauchlan, K. K., Higuera, P. E., Gavin, D. G., Perakis, S. S., Mack, M. C., Alexander, H., Battles, J., Biondi, F., Buma, B., Colombaroli, D., Enders, S. K., Engstrom, D. R., Hu, F. S., Marlon, J. R., Marshall, J., McGlone, M., Morris, J. L., Nave, L. E., Shuman, B., … Williams, J. J. (2014). Reconstructing disturbances and their biogeochemical consequences over multiple timescales. *BioScience*, *64*(2), 105–116. https://doi.org/10.1093/biosci/bit017

McLauchlan, K. K., Higuera, P. E., Miesel, J., Rogers, B. M., Schweitzer, J., Shuman, J. K., Tepley, A. J., Varner, J. M., Veblen, T. T., Adalsteinsson, S. A., Balch, J. K., Baker, P., Batllori, E., Bigio, E., Brando, P., Cattau, M., Chipman, M. L., Coen, J., Crandall, R., … Watts, A. C. (2020). Fire as a fundamental ecological process: Research advances and frontiers. *Journal of Ecology*, *108*, 2047–2069. https://doi.org/10.1111/1365-2745.13403

Meyers, P. A. (1997). Organic geochemical proxies of paleoceanographic, paleolimnologic, and paleoclimatic processes. *Organic Geochemistry*, *27*(5–6), 213–250. https://doi.org/10.1016/S0146-6380(97)00049-1

Meyers, P. A., & Teranes, J. L. (2001). Sediment organic matter. In *Tracking environmental change using lake sediments: Physical and geochemical methods* (Vol. *2*, 1st ed., pp. 239–269). Kulwer Academic Publishers.

Morgan, P., Heyerdahl, E. K., & Gibson, C. E. (2008). Multi-season climate synchronized fires throughout the 20th century, northern Rockies, USA. *Ecology*, *89*(3), 717–728. https://doi.org/10.1890/06-2049.1

Morris, D. P., & Lewis, W. M. (1988). Phytoplankton nutrient limitation in Colorado mountain lakes. *Freshwater Biology*, *20*(3), 315–327. https://doi.org/10.1111/j.1365-2427.1988.tb00457.x

Morris, J. L., McLauchlan, K. K., & Higuera, P. E. (2015). Sensitivity and complacency of sedimentary biogeochemical records to climate-mediated forest disturbances. *Earth-Science Reviews*, *148*, 121–133. https://doi.org/10.1016/j.earscirev.2015.06.001

Muff, S., Nilsen, E. B., O'Hara, R. B., & Nater, C. R. (2021). Rewriting results sections in the language of evidence. *Trends in Ecology & Evolution*, *37*, 203–210. https://doi.org/10.1016/j.tree.2021.10.009

Murtagh, F., & Legendre, P. (2014). Ward's hierarchical agglomerative clustering method: Which algorithms implement Ward's criterion? *Journal of Classification*, *31*(3), 274–295. https://doi.org/10.1007/s00357-014-9161-z

Napier, J. D., & Chipman, M. L. (2022). Emerging palaeoecological frameworks for elucidating plant dynamics in response to fire and other disturbance. *Global Ecology and Biogeography*, *31*(1), 138–154. https://doi.org/10.1111/geb.13416

Oris, F., Asselin, H., Finsinger, W., Hély, C., Blarquez, O., Ferland, M.-E., Bergeron, Y., & Ali, A. A. (2014). Long-term fire history in northern Quebec: Implications for the northern limit of commercial forests. *Journal of Applied Ecology*, *51*(3), 675–683. https://doi.org/10.1111/1365-2664.12240

Parish, M. C., Wolf, K. D., Higuera, P. E., & Shuman, B. N. (2022). Holocene water levels of Silver Lake, Montana, and the hydroclimate history of the inland northwest. *Quaternary Research*, *110*, 54–66. https://doi.org/10.1017/qua.2022.17

Parks, S. A., Miller, C. L., Abatzoglou, J., Holsinger, L. M., Parisien, M. A., & Dobrowski, S. (2016). How will climate change affect wildland fire severity in the western US? *Environmental Research Letters*, *11*(3), 35002. https://doi.org/10.1088/1748-9326/11/3/035002

Pellegrini, A. F. A., Ahlström, A., Hobbie, S. E., Reich, P. B., Nieradzik, L. P., Staver, A. C., Scharenbroch, B. C., Jumpponen, A., Anderegg, W. R. L., Randerson, J. T., & Jackson, R. B. (2018). Fire frequency drives decadal changes in soil carbon and nitrogen and ecosystem productivity. *Nature*, *553*, 194–198. https://doi.org/10.1038/nature24668

Pellegrini, A. F. A., Hobbie, S. E., Reich, P. B., Jumpponen, A., Brookshire, E. N. J., Caprio, A. C., Coetsee, C., & Jackson, R. B. (2020). Repeated fire shifts carbon and nitrogen cycling by changing plant inputs and soil decomposition across ecosystems. *Ecological Monographs*, *90*(4), e01409. https://doi.org/10.1002/ECM.1409

Perakis, S. S., Tepley, A. J., & Compton, J. E. (2015). Disturbance and topography shape nitrogen availability and δ^{15}N over long-term forest succession. *Ecosystems*, *18*(4), 573–588. https://doi.org/10.1007/s10021-015-9847-z

Pompeani, D. P., McLauchlan, K. K., Chileen, B. V., Calder, W. J., Shuman, B. N., & Higuera, P. E. (2020). The biogeochemical consequences of late Holocene wildfires in three subalpine lakes from northern Colorado. *Quaternary Science Reviews*, *236*, 106293. https://doi.org/10.1016/j.quascirev.2020.106293

PRISM Climate Group (Oregon State University). (2021). *PRISM 30-year normals* [dataset]. Oregon State University. http://prism.oregonstate.edu

R Core Team. (2021). *R: A language and environment for statistical computing*. (4.1.1) [Computer software].

Raison, R. J. (1979). Modification of the soil environment by vegetation fires, with particular reference to nitrogen transformations: A review. *Plant and Soil*, *51*(1), 73–108.

Reimer, P. J., Austin, W. E. N., Bard, E., Bayliss, A., Blackwell, P. G., Ramsey, C. B., Butzin, M., Cheng, H., Edwards, R. L., Friedrich, M., Grootes, P. M., Guilderson, T. P., Hajdas, I., Heaton, T. J., Hogg, A. G., Hughen, K. A., Kromer, B., Manning, S. W., Muscheler, R., … Talamo, S. (2020). The IntCal20 northern hemisphere radiocarbon age calibration curve (0–55 cal kBP). *Radiocarbon*, *62*(4), 725–757. https://doi.org/10.1017/RDC.2020.41

Rhoades, C. C., Entwistle, D., & Butler, D. (2011). The influence of wildfire extent and severity on streamwater chemistry, sediment and temperature following the Hayman Fire, Colorado. *International Journal of Wildland Fire*, *20*(3), 430–442. https://doi.org/10.1071/WF09086

Robinson, D. (2001). Δ^{15}N as an integrator of the nitrogen cycle. *Trends in Ecology & Evolution*, *16*(3), 153–162. https://doi.org/10.1016/S0169-5347(00)02098-X

Seidl, R., & Turner, M. G. (2022). Post-disturbance reorganization of forest ecosystems in a changing world. *Proceedings of the National Academy of Sciences of the United States of America*, *119*(28), e2202190119. https://doi.org/10.1073/pnas.2202190119

Shakesby, R. A., & Doerr, S. H. (2006). Wildfire as a hydrological and geomorphological agent. *Earth-Science Reviews*, *74*(3–4), 269–307. https://doi.org/10.1016/j.earscirev.2005.10.006

Smithwick, E. A. H. (2011). Pyrogeography and biogeochemical resilience. In D. McKenzie, C. Miller, & D. A. Falk (Eds.), *The landscape ecology of fire* (pp. 143–163). Springer Netherlands. https://doi.org/10.1007/978-94-007-0301-8_6

Smithwick, E. A. H., Turner, M. G., Mack, M. C., & Chapin, F. S. (2005). Postfire soil N cycling in northern conifer forests affected by severe, stand-replacing wildfires. *Ecosystems*, *8*(2), 163–181. https://doi.org/10.1007/s10021-004-0097-8

Spencer, C. N., Gabel, K. O., & Hauer, F. R. (2003). Wildfire effects on stream food webs and nutrient dynamics in Glacier National Park, USA. *Forest Ecology and Management*, *178*(1), 141–153. https://doi.org/10.1016/S0378-1127(03)00058-6

Talbot, M. R. (2001). Nitrogen isotopes in palaeolimnology. In *Tracking environmental change using lake sediments: Physical and geochemical methods* (Vol. *2*, 1st ed., pp. 401–439). Kulwer Academic Publishers.

The MathWorks, Inc. (2021). *MATLAB* (9.11.0 (R2021b)) [Computer software].

Tierney, J. A., Hedin, L. O., & Wurzburger, N. (2019). Nitrogen fixation does not balance fire-induced nitrogen losses in longleaf pine savannas. *Ecology*, *100*(7), e02735. https://doi.org/10.1002/ecy.2735

Toberman, H., Chen, C., Lewis, T., & Elser, J. J. (2014). High-frequency fire alters C:N:P stoichiometry in forest litter. *Global Change Biology*, *20*(7), 2321–2331. https://doi.org/10.1111/gcb.12432

Turner, M. G., Braziunas, K. H., Hansen, W. D., & Harvey, B. J. (2019). Short-interval severe fire erodes the resilience of subalpine lodgepole pine forests. *Proceedings of the National Academy of Sciences of the United States of America*, *166*(23), 11319–11328. https://doi.org/10.1073/pnas.1902841116

Turner, M. G., Smithwick, E. A. H., Metzger, K. L., Tinker, D. B., & Romme, W. H. (2007). Inorganic nitrogen availability after severe stand-replacing fire in the Greater Yellowstone ecosystem. *Proceedings of the National Academy of Sciences of the United States of America*, *104*(12), 4782–4789. https://doi.org/10.1073/pnas.0700180104

USDA-NRCS, University of California, Davis, C. S. R. L., & University of California, D. of A. and N. R. (2019). *SoilWeb: Online soil survey*. University of California; Natural Resouces Conservation Service. https://data.nal.usda.gov/dataset/soilweb

Vieira, D. C. S., Fernández, C., Vega, J. A., & Keizer, J. J. (2015). Does soil burn severity affect the post-fire runoff and interrill erosion response? A review based on meta-analysis of field rainfall simulation data. *Journal of Hydrology*, *523*, 452–464. https://doi.org/10.1016/j.jhydrol.2015.01.071

Vitousek, P. M., & Reiners, W. A. (1975). Ecosystem succession and nutrient retention: A hypothesis. *BioScience*, *25*(6), 376–381. https://doi.org/10.2307/1297148

Vuke, S. M., Porter, K. W., Lonn, J. D., & Lopez, D. A. (2007). *Geologic map of Montana* [geologic map]. U.S. Geological Survey, Montana Bureau of Mines and Geology.

Walker, X. J., Baltzer, J. L., Cumming, S. G., Day, N. J., Ebert, C., Goetz, S., Johnstone, J. F., Potter, S., Rogers, B. M., Schuur, E. A. G., Turetsky, M. R., & Mack, M. C. (2019). Increasing wildfires threaten historic carbon sink of boreal forest soils. *Nature*, *572*(7770), 520–523. https://doi.org/10.1038/s41586-019-1474-y

Walker, X. J., Rogers, B. M., Veraverbeke, S., Johnstone, J. F., Baltzer, J. L., Barrett, K., Bourgeau-Chavez, L., Day, N. J., de Groot, W. J., Dieleman, C. M., Goetz, S., Hoy, E., Jenkins, L. K., Kane, E. S., Parisien, M.-A., Potter, S., Schuur, E. A. G., Turetsky, M., Whitman, E., & Mack, M. C. (2020). Fuel availability not fire weather controls boreal wildfire severity and carbon emissions. *Nature Climate Change*, *10*(12), 1130–1136. https://doi.org/10.1038/s41558-020-00920-8

Wan, S., Hui, D., & Luo, Y. (2001). Fire effects on nitrogen pools and dynamics in terrestrial ecosystems: A meta-analysis. *Ecological Applications*, *11*(5), 1349–1365. https://doi.org/10.1890/1051-0761(2001)011[1349:feonpa]2.0.co;2

Westerling, A. L. (2016). Increasing western US forest wildfire activity: Sensitivity to changes in the timing of spring. *Philosophical Transactions of the Royal Society of London. Series B, Biological Sciences*, *371*(1696), 20150178. https://doi.org/10.1098/rstb.2015.0178

Whitlock, C., & Larsen, C. (2001). Charcoal as a fire proxy. In J. P. Smol, H. J. B. Birks, & W. M. Last (Eds.), *Tracking environmental change using lake sediments. Volume 3: Terrestrial, algal, and siliceous indicators* (pp. 75–97). Kluwer Academic Publishers.

Wright, H. E., Mann, D. H., & Glaser, P. H. (1984). Piston corers for peat and lake sediments. *Ecology*, *65*(2), 657–659.

Yelenik, S., Perakis, S., & Hibbs, D. (2013). Regional constraints to biological nitrogen fixation in post-fire forest communities. *Ecology*, *94*(3), 739–750. https://doi.org/10.1890/12-0278.1

Zhuang, Y., Fu, R., Santer, B. D., Dickinson, R. E., & Hall, A. (2021). Quantifying contributions of natural variability and anthropogenic forcings on increased fire weather risk over the western United States. *Proceedings of the National Academy of Sciences of the United States of America*, *118*(45), e2111875118. https://doi.org/10.1073/pnas.2111875118

SUPPORTING INFORMATION

Additional supporting information can be found online in the Supporting Information section at the end of this article.

Appendix S1. Supplementary methods.

Appendix S2. Supplementary results.

Table S1. Dates used to construct the Silver Lake chronology.

Table S2. Zones used to test changes in fire frequency, giving estimated mean fire return intervals (mFRI) and 95% confidence intervals for the mean.

Figure S1. Age–depth relationship over the past 7600 years for the Silver Lake core.

Figure S2. Local palaeoclimate history from Silver Lake and regional vegetation history from Dismal Lake, ID.

Figure S3. Fire history from Silver Lake over the past 4800 years.

Figure S4. C:N ratios and stable isotope measurements of lake-sediment samples spanning the past 4800 years at Silver Lake and modern terrestrial soil and foliar samples from the surrounding watershed.

Figure S5. Charcoal peak magnitude (number of charcoal pieces cm^{-2} $peak^{-1}$) and fire response type over time.

Figure S6. Boxplots comparing pollen ratios and pollen abundances of major taxa among samples grouped by coincidence with fire.

Figure S7. Ratio of Fe to Mn in lake sediments from Silver Lake and reconstructed water depth over the past 4800 years.

Figure S8. Time series of charcoal accumulation and magnetic susceptibility (MS).

How to cite this article: Clark-Wolf, K. D., Higuera, P. E., McLauchlan, K. K., Shuman, B. N., & Parish, M. C. (2023). Fire-regime variability and ecosystem resilience over four millennia in a Rocky Mountain subalpine watershed. *Journal of Ecology*, *00*, 1–19. https://doi.org/10.1111/1365-2745.14201